

The amyloid precursor protein is a conserved Wnt receptor

Tengyuan Liu^{1,2}, Tingting Zhang^{1,2}, Maya Nicolas^{2,3,4†}, Lydie Boussicault¹, Heather Rice^{3,4‡}, Alessia Soldano^{3,4§}, Annelies Claeys^{3,4}, Iveta Petrova⁵, Lee Fradkin⁵, Bart De Strooper^{3,6}, Marie-Claude Potier¹, Bassem A Hassan^{1*}

¹Paris Brain Institute – Institut du Cerveau, Sorbonne Université, Inserm, CNRS, Hôpital Pitié-Salpêtrière, Paris, France; ²Doctoral School of Biomedical Sciences, Leuven, Belgium; ³Center for Brain and Disease, Leuven, Belgium; ⁴Center for Human Genetics, University of Leuven School of Medicine, Leuven, Belgium; ⁵Laboratory of Developmental Neurobiology, Department of Molecular Cell Biology, Leiden University Medical Center, Leiden, Netherlands; ⁶UK Dementia Research institute at University College London, London, United Kingdom

***For correspondence:**

bassem.hassan@icm-institute.org

Present address: [†]School of Sciences and Engineering, The American University in Cairo, Cairo, Egypt; [‡]Department of Biochemistry and Molecular Biology, Oklahoma Center for Geroscience and Healthy Brain Aging, University of Oklahoma Health Sciences Center, Oklahoma, United States; [§]Laboratory of Translational Genomics, Department of Cellular, Computational and Integrative Biology (CIBIO), University of Trento, Trento, Italy

Competing interests: The authors declare that no competing interests exist.

Funding: See page 22

Received: 09 April 2021

Accepted: 01 September 2021

Published: 09 September 2021

Reviewing editor: Hugo J Bellen, Baylor College of Medicine, United States

© Copyright Liu et al. This article is distributed under the terms of the [Creative Commons Attribution License](https://creativecommons.org/licenses/by/4.0/), which permits unrestricted use and redistribution provided that the original author and source are credited.

Abstract The Amyloid Precursor Protein (APP) and its homologues are transmembrane proteins required for various aspects of neuronal development and activity, whose molecular function is unknown. Specifically, it is unclear whether APP acts as a receptor, and if so what its ligand(s) may be. We show that APP binds the Wnt ligands Wnt3a and Wnt5a and that this binding regulates APP protein levels. Wnt3a binding promotes full-length APP (flAPP) recycling and stability. In contrast, Wnt5a promotes APP targeting to lysosomal compartments and reduces flAPP levels. A conserved Cysteine-Rich Domain (CRD) in the extracellular portion of APP is required for Wnt binding, and deletion of the CRD abrogates the effects of Wnts on flAPP levels and trafficking. Finally, loss of APP results in increased axonal and reduced dendritic growth of mouse embryonic primary cortical neurons. This phenotype can be cell-autonomously rescued by full length, but not CRD-deleted, APP and regulated by Wnt ligands in a CRD-dependent manner.

Introduction

The Amyloid Precursor Protein (APP) is the precursor that generates the A β peptide, whose accumulation is associated with Alzheimer's disease (AD; *Selkoe and Hardy, 2016*). As an ancient and highly conserved protein, APP and its homologs are found across animal species in both vertebrates and invertebrates (*Shariati and De Strooper, 2013*). As a result of the alternative splicing of the 18 exons coding for APP, there are three major isoforms expressed in different organs or tissues in mice and human (*Panegyres and Atkins, 2011*). APP695 is the major isoform expressed in the brain (*Kang et al., 1987*). The expression of APP is detected at early stage during development (*Ott and Bullock, 2001; Sarasa et al., 2000*). In the developing mouse cortex, App mRNA is expressed continuously starting at embryonic day 9.5 (E9.5) coinciding with the initiation of neurogenesis and neuronal differentiation (*Salbaum and Ruddle, 1994*).

Structurally, APP is a type I transmembrane protein, which possesses a large extracellular amino acids sequence, an α -helix transmembrane sequence and a relatively short intracellular C-terminal sequence (*Müller and Zheng, 2012; Coburger et al., 2013*). Based on the architecture of the ectodomain, APP has been proposed to be a putative receptor (*Ninomiya et al., 1993; Pietrzik et al., 2004; Hoe et al., 2009; Chen et al., 2006; Deyts et al., 2016*). APP trafficking and processing have been intensively studied ever since the protein was first cloned. The turnover of transmembrane full-length APP is rapid (*Hunter and Brayne, 2012; El Ayadi et al., 2012*), and internalised APP can be degraded in lysosome or processed by α -, β -, and γ -secretase in different subcellular compartments

to produce corresponding segments of APP. (Haass et al., 2012; Yuksel and Tacal, 2019). Recently, effort has been put into researching the function of the proteolytic products of APP under normal physiological condition (Coronel et al., 2018), as this may provide new clues for AD research.

During *Drosophila* brain development the fly homolog of APP, called APPL, functions as key component of the neuronal Wnt-PCP signaling pathway and regulates the axonal outgrowth in fly mushroom body (Soldano et al., 2013). Both mammalian APP and fly APPL contain a Cysteine-Rich Domain (CRD) in the ectodomain of APP whose Cysteine distribution resembles that of the Wnt Tyrosine-protein kinase receptor Ror2 (Coburger et al., 2013; Oishi et al., 2003), suggesting the intriguing possibility that APP may itself be a receptor for Wnt family member.

Wnt signaling is an evolutionary conserved signal transduction pathway that regulates a large number of cellular processes. Three Wnt signaling pathway have been well described: the β -catenin-based canonical pathway, the planar cell polarity (PCP/Wnt) signaling pathway and the calcium pathway. Wnt signaling regulates various features during development such as cell proliferation, migration, and differentiation (Eisenmann, 2005). Recently, increasing evidence indicates that the Wnt signaling pathways are involved in the APP-related A β production (Sellers et al., 2018; Elliott et al., 2018), but the precise mode of interaction between APP and the various Wnt pathways remains unclear.

The presence of CRD in APP, the reported involvement of Wnt signaling in APP processing and the importance of Wnt signaling during development suggested to us that APP may be a novel class of Wnt receptor regulating neuronal development. We used *Drosophila* and mouse embryonic primary cortical neurons as models to explore the APP-Wnt interactions during development. We provide evidence that the CRD of APP is a conserved binding domain for both canonical and PCP Wnt ligands. Furthermore, APP trafficking and expression is regulated by Wnts through the CRD, which in turn is required for APP to regulate axonal and dendritic growth and branching.

Results

Drosophila APP like interacts genetically with Wnt5

Drosophila APPL has been implicated in neural development (Cassar and Kretzschmar, 2016; Nicolas and Hassan, 2014) and is required for learning and memory (Preat and Goguel, 2016). *Drosophila* APPL is a homologue of human APP and has been used as a model for understanding the physiological function of the APP family (Soldano and Hassan, 2014; van der Kant and Goldstein, 2015). We previously reported that *appl* genetically interacts with components of the Wnt-PCP pathway (Soldano et al., 2013) during mushroom body (MB) axon growth. The MBs are a bilateral neuronal structure in the fly brain required for learning and memory (Heisenberg, 2003). To understand the role of APPL in axonal PCP signaling, we first explored the specific nature of the genetic interaction between *appl* and the gene encoding the PCP protein Van Gough (Vang). In contrast to control MBs, 17% of male *appl* null mutant flies (*appl*^{d/Y}, henceforth *Appl*^{-/-}) displayed a loss of the MBb-lobe (Figure 1A,A'). The PCP receptor Vang is also required for β -lobe growth (Shimizu et al., 2011); we observed that flies homozygous for the null allele *vang*^{stbm-6} exhibited 50% β -lobe loss. Whereas *vang*^{stbm-6} heterozygotes show no MB defects, the loss of one copy of *vang* in *Appl*^{-/-} flies is comparable (43% β -lobe loss) to the complete loss of *vang* (Figure 1B). Therefore, in the absence of *appl*, *vang* is haploinsufficient. Next, we performed rescue experiments of *Appl*^{-/-} mutant flies. Re-expression of APPL in the mutant MBs significantly rescued β -lobe loss. In contrast, the overexpression of Vang in *Appl*^{-/-} null flies failed to do so. These loss and gain of function data suggest that Wnt-PCP signaling requires APPL to regulate axonal growth (Figure 1B).

APPL and Vang are both transmembrane proteins that are part of the same receptor complex required for MB axonal growth (Soldano et al., 2013). We wondered if APPL interaction with the Wnt-PCP pathway involved a ligand and focused on *Drosophila* Wnt5 as a candidate. Wnt5 has been implicated in the regulation of MB axon growth (van der Kant and Goldstein, 2015; Grillenzoni et al., 2007), although the mechanism is unclear. We first examined the genetic interaction between Wnt5 and *vang* in β -lobe axon growth. Loss of *vang* caused a highly penetrant phenotype (50%), while Wnt5 nulls showed β -lobe loss only in 5% of the brains examined, suggesting that Wnt5 is largely dispensable for β -lobe growth. Surprisingly, *Wnt5*^{-/-}; *vang*^{-/-} double mutants showed an almost complete rescue of *vang* loss of function (Figure 1C a,b,d,D, Supplementary file 1).

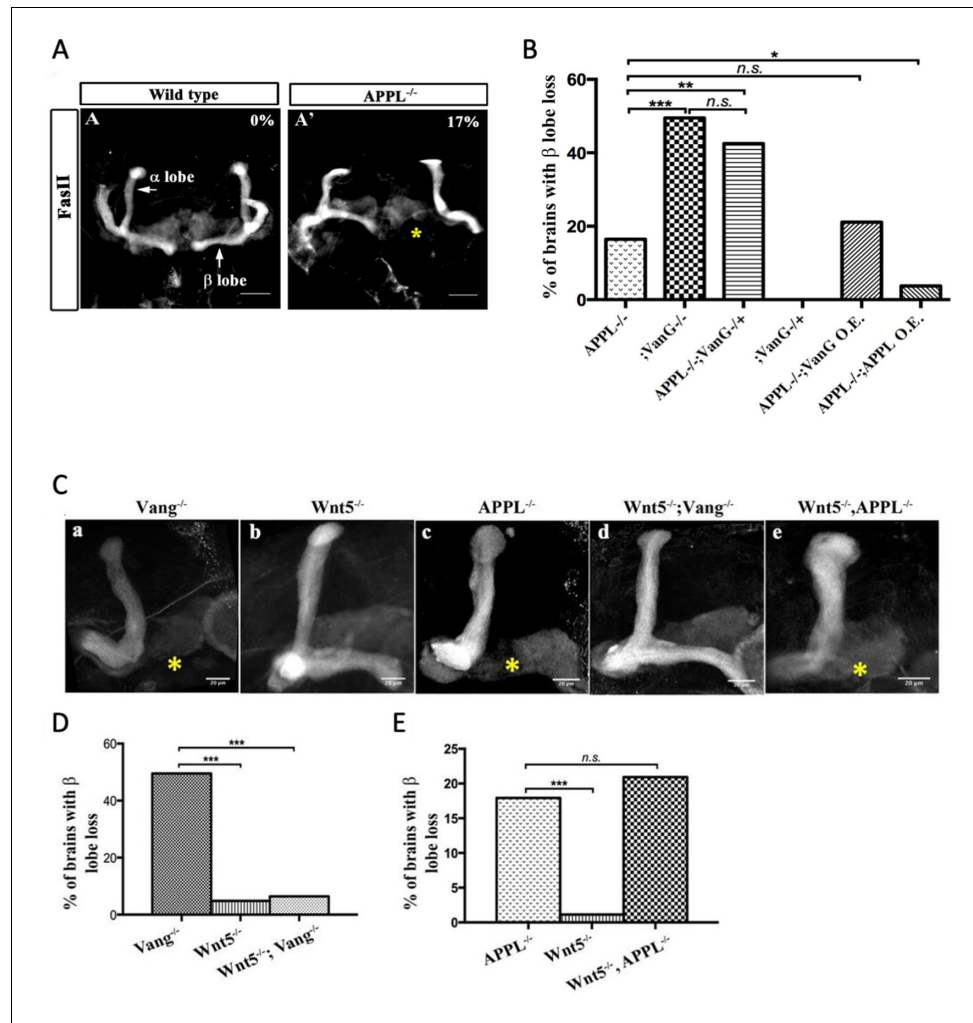


Figure 1. APPL mediates Wnt5a function in axonal growth. (A–A') Structure of the MB neurons in adult wild type and APPL^{-/-} mutant flies. Immunofluorescence using anti-FasII (FasII) antibody that labels the axons of the MB. (A) In wild type brains, the axons of the MB project dorsally to form the α lobe and medially to form the β lobe. (A') In APPL null mutant flies (APPL^{Δ/Y} referred to as APPL^{-/-}), there is axonal growth defect of the β lobe (as indicated by the asterisk) in 17% of the brains examined (n=97). Images are z-projections of confocal image stacks (scale bar, 50 μm). (B) APPL and Vang synergistically interact and APPL is necessary for Vang activity. The histogram shows the percentage of the β lobe defect in different genetic backgrounds. The loss of Vang induced a significantly higher penetrant phenotype up to 50%, (n=103) compared to APPL^{-/-}; p value = 5.18⁻⁷ calculated with G-test. The loss of one copy of Vang in wild type background had no effect on axonal growth (n=30). However, the removal of one copy of Vang in APPL^{-/-} background significantly increased the phenotype to 43% (n=47) compared to APPL^{-/-}; p value = 0.001026. The penetrance of the latter phenotype was not significantly different from the one observed in Vang^{-/-}; p value = 0.4304. While the overexpression of APPL rescued the APPL^{-/-} phenotype (4%, n=54); p value = 0.01307, the overexpression of Vang failed to (21%, n=52); p value = 0.4901. * Indicates a p value < 0.05. Data are shown as median ± whiskers. (C–e) Immunofluorescence analysis using anti-FasII antibody to show the structure of the MB axons in adult mutant flies of the following genotypes: (a) Vang^{-/-}, (b) Wnt5^{Δ/Y} referred to as Wnt5^{-/-}, (c) APPL^{-/-}, (d) Wnt5^{-/-};Vang^{-/-}, and (e) Wnt5^{-/-};APPL^{-/-}. Images are z-projections of confocal image stacks (scale bar, 20 μm). The asterisks correspond to the β lobe loss phenotype. (D) Wnt5 inhibits axonal growth, after branching, independently of Vang. The Histogram shows the percentage of the β lobe loss phenotype. Vang^{-/-} flies exhibit a highly penetrant phenotype of 50% (n=104), while Wnt5^{-/-} flies show a significantly less penetrant phenotype (5%, n=103); p value = 2.33⁻¹⁴ calculated with G-test. The loss of Wnt5 rescued Vang loss of function (6%, n=98); p value = 4.56⁻¹². (E) Wnt5 inhibits axonal growth probably through APPL. Histogram showing the penetrance of the β lobe loss phenotype. In APPL^{-/-} flies, 18% of the brains tested showed an axonal defect (n=106). This percentage did not significantly change in the absence of both Wnt5 in APPL^{-/-} flies (21%, n=86); p value = 0.6027. *** indicates a p value < 1⁻⁵.

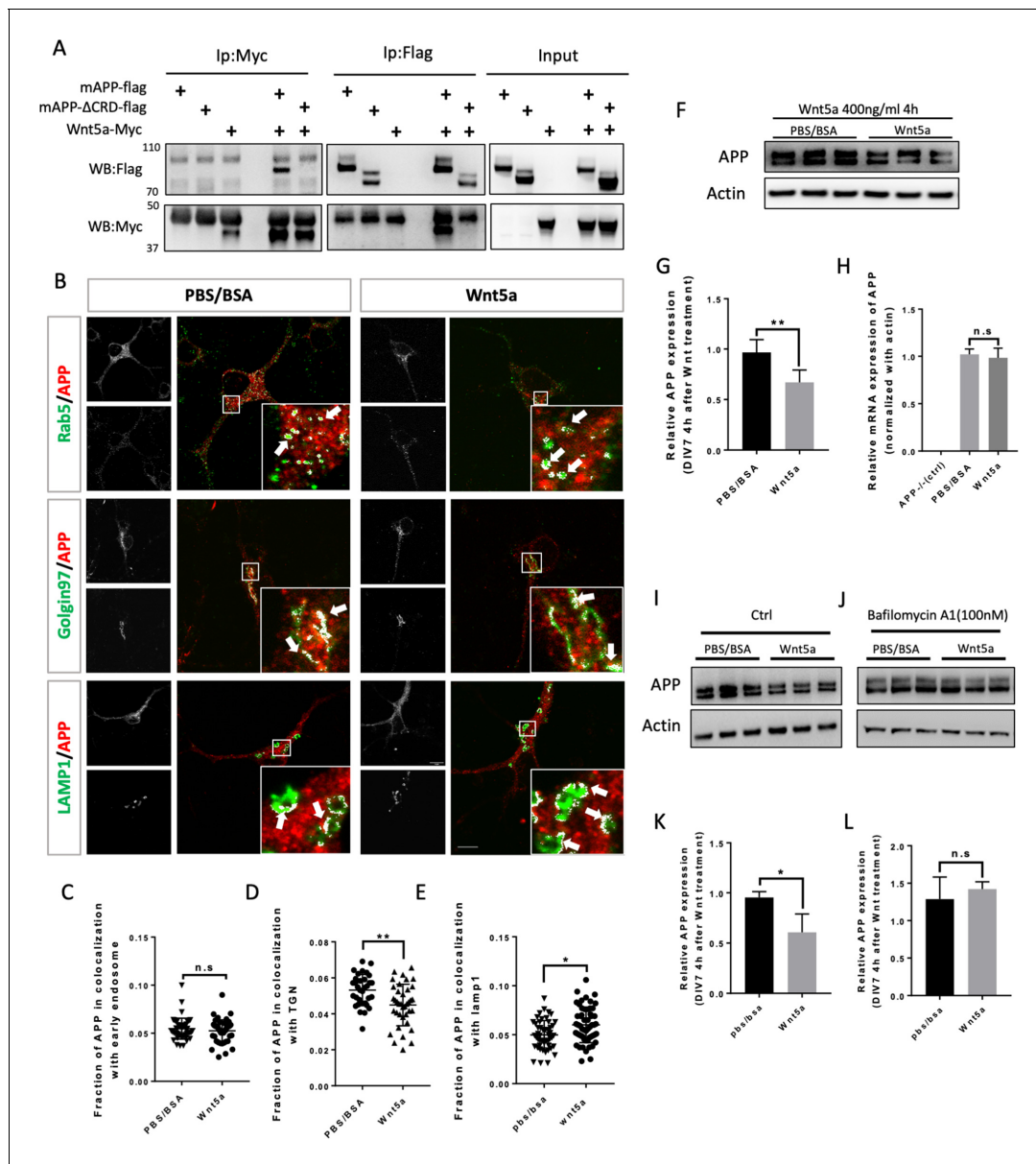


Figure 3. Wnt5a regulates APP expression through changing its intracellular trafficking. **(A)** Co-immunoprecipitation (co-IP) of Wnt5a-Myc with full-length proteins mAPP-flag or mAPP-delatCRD-flag. The tagged proteins were co-expressed in HEK293T cells and immunoprecipitated with anti-flag and anti-Myc antibodies. Wild-type mAPP could pull down Wnt5a and vice versa, while mAPP lacking the CRD domain showed impaired ability to pull down Wnt5a, even with higher protein levels compared to wild-type mAPP in the input. **(B)** mAPP localization after 4 hr PBS/BSA or Wnt5a treatment. Immunofluorescence for APP (red), Rab5 (early endosome marker, green), Golgin97 (TGN marker, green), and Lamp1 (lysosome marker, green) revealed mAPP localization in different intracellular compartments. The inset showed zoomed in images of the area in the white box and arrows indicated the overlap of mAPP with respective cellular compartment markers. Scale bar = 10 μ m. **(C–E)** Quantification of the overlap of mAPP with early endosome **(C)**, TGN **(D)** or lysosome **(E)**, respectively, after Wnt5a treatment. (n=33–55 cells, t-test). **(F)** Western blots of mAPP and Actin on the lysates of DIV7 primary cultured cortical neurons showed that mAPP protein expression level was altered after Wnt5a treatment. **(G)** Quantification of the western blots results for fig F. (n=three biological independent repeat, t-test). **(H)** qPCR results showed that *mApp* mRNA expression was not affected after Wnt5a treatment on DIV7. *App*^{-/-} mice derived primary neurons were used as a negative control. (n=three biological independent repeat, one-way ANOVA). **(I and J)** Western blots for APP showed that the lysosome inhibitor Bafilomycin-A **(J)** could rescue Wnt5a-induced mAPP reduction compared with control groups **(I)**. **(K and L)** Quantification of the western blots result for figure I and J. (n=three biological independent repeat, t-test). Bars represent the mean \pm S.E.M. Samples collected from at least two independent experiments. *p<0.05, **p<0.01. .

The online version of this article includes the following source data and figure supplement(s) for figure 3:

Source data 1. Co-immunoprecipitation (co-IP) of Wnt5a-Myc with full-length proteins mAPP-flag or mAPP-delatCRD-flag.

Source data 2. Western blots for mAPP and Actin after Wnt5a treatment on DIV7 primary cortical neurons.

Figure 3 continued on next page

Figure 3 continued

Source data 3. Western blots for mAPP and Actin after Wnt5a treatment on DIV7 primary cortical neurons.

Source data 4. Western blots for mAPP and Actin after adding Bafilomycin followed by Wnt5a treatment on DIV7 primary cortical neurons.

Figure supplement 1. Rapid turnover of fl-mAPP in culture mouse primary cortical neurons.

Figure supplement 1—source data 1. Western blots for time course (0.5 hr, 1 hr, 2 hr, 4 hr) of fl-mAPP expression after Cycloheximide (50 µg/ml) treatment on DIV7 primary cortical neurons.

Figure supplement 1—source data 2. Western blots for time course (0.5 hr, 1 hr, 2 hr, 4 hr) of fl-mAPP expression after DMSO (0.05%), treatment on DIV7 primary cortical neurons.

Figure supplement 2. APP overlap with early endosome, TGN and lysosome after Wnt3a/5a treatment.

Figure supplement 3. Wnt3a/5a treatment barely affect APP overlap with recycling endosome.

Figure supplement 4. Rab5 Golgin97 and Lamp1 expression after Wnt3a/5a treatment.

Figure supplement 4—source data 1. Western blots for fl-mAPP, Rab5, Golgin97, and Lamp1 after 4 hr of Wnt3a/5a treatment on DIV7 primary cortical neurons.

Figure supplement 5. Time course of fl-mAPP after Wnt3a/5a treatment.

Figure supplement 5—source data 1. Representative western blots for the time course (0.5 hr, 1 hr, 2 hr, 4 hr) of fl-mAPP expression after PBS/BSA (ctrl) and Wnt3a/5a treatment at DIV7.

performed co-immunoprecipitation (IP) assays. Wnt5a immunoprecipitated full-length hAPP and APPL but not hAPP Δ CRD or APPL Δ CRD (**Figure 2B**). Reciprocally, full-length hAPP and APPL immunoprecipitated significant amounts of Wnt5a in contrast to hAPP Δ CRD and APPL Δ CRD (**Figure 2B'**). Similarly, APPL was found to precipitate Wnt5 from transfected *Drosophila* S2 cell lysates (**Figure 2—figure supplement 2**).

Wnt5a treatment affects APP trafficking and expression in maturing mouse primary cortical neuron

The findings above suggest that the APP family may represent a new class of conserved Wnt receptors. We sought to investigate this further at a cell biological level using developing mouse embryonic primary cortical neurons as a model system. APP trafficking and processing have been intensively investigated in studies relating to AD, and according to early reports the half-life of APP is quite short, ranging from 1 hr to 4 hr (**Hunter and Brayne, 2012; El Ayadi et al., 2012**). In mouse embryonic (E16) primary neuron cultures, full-length mouse APP (fl-mAPP; henceforth we refer to mouse APP as mAPP and to human APP as hAPP) expression significantly dropped after 2 hr of treatment with translational inhibitor (Cycloheximide) (**Figure 3—figure supplement 1**), suggesting relatively rapid turnover of mAPP. To study the relation between mAPP and Wnts, we first verified that mAPP also binds Wnt5a through its CRD and found that fl-mAPP but not mAPP Δ CRD co-IP's with Wnt5a, similar to APPL and hAPP (**Figure 3A**). Next, we used immunofluorescence to localize mAPP with or without Wnt5a treatment in developing cortical neurons during axonal outgrowth (DIV7). mAPP is modified to maturation in the Trans Golgi Network (TGN) to be subsequently transferred to the plasma membrane where it can be internalized into early endosomes. From the early endosome, mAPP is either recycled back to the TGN through retromer-dependent sorting, or to the late endosome and then lysosome to be degraded (**Haass et al., 2012; Vagnozzi and Praticò, 2019**). We used markers for early endosomes (Rab5), recycling endosome (Rab11), TGN (Golgin97), and lysosomes (Lamp1) to trace mAPP trafficking after 2 hr and 4 hr Wnt5a treatment. The fraction of mAPP co-localized with early endosomes was not affected after 2 hr (**Figure 3—figure supplement 2A**) or 4 hr (**Figure 3B,C**) of Wnt5a treatment. Similarly, we observed no effects on co-localization with recycling endosomes (**Figure 3—figure supplement 3A,D**) indicating normal initial internalization and recycling of mAPP. However, we found a reduction of mAPP in the TGN, accompanied by an increase of mAPP in lysosomes both after 2 hr (**Figure 3—figure supplement 2D,G**) and 4 hr (**Figure 3B,D,E**) of Wnt5a treatment suggesting that Wnt5a regulates intracellular targeting of mAPP after internalization. Importantly, the levels of expression of these markers (Rab5, Golgin97, and Lamp1) are not affected by Wnt5a treatment (**Figure 3—figure supplement 4**). Next, we asked if this altered trafficking affected mAPP levels. We found that the level of fl-mAPP was significantly reduced after 4 hr of Wnt5a treatment, as shown by western blot (**Figure 3F,G**), with no effect on mApp mRNA levels (**Figure 3H**). The results of immunofluorescence (IF) and western blot (WB) suggest that the decrease of the mAPP upon Wnt5a treatment is caused by lysosomal degradation. To

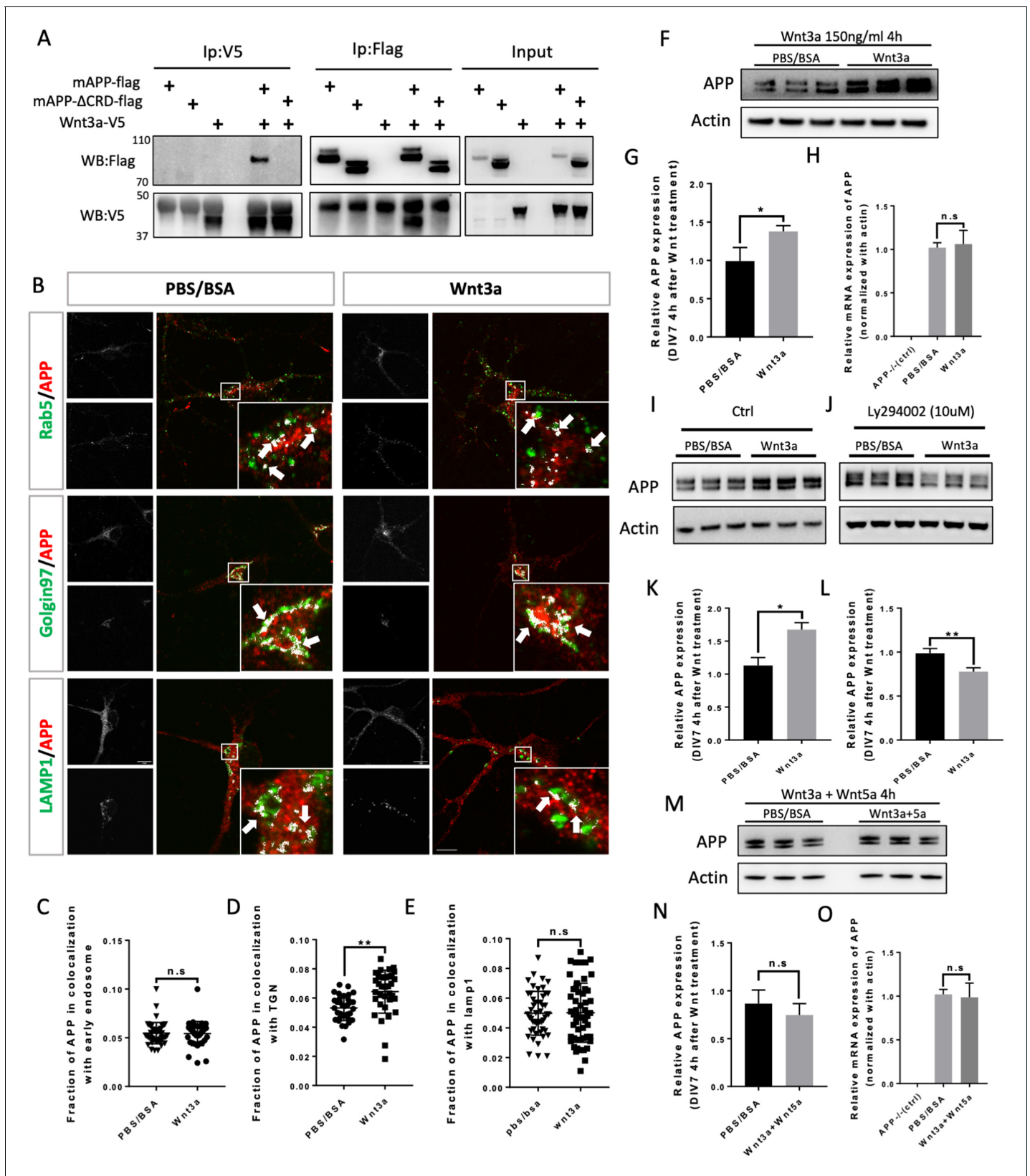


Figure 4. Wnt3a binds to and regulates APP expression through changing its intracellular trafficking. (A) Co-immunoprecipitation (co-IP) of Wnt3a-V5 with full-length proteins mAPP-flag or mAPP-ΔCRD. The tagged proteins were co-expressed in HEK293T cells and immunoprecipitated with anti-flag and anti-v5 antibodies. Wild-type mAPP could pull down Wnt3a and vice versa, while mAPP lacking the CRD domain showed impaired ability to pull down Wnt3a. (B) Immunofluorescence images showing the localization of APP (red) with Rab5 (green), Golgin97 (green), and LAMP1 (green) in HEK293T cells treated with PBS/BSA or Wnt3a. White arrows indicate colocalization. (C-E) Dot plots showing the fraction of APP in colocalization with early endosome (C), TGN (D), and LAMP1 (E) in cells treated with PBS/BSA or Wnt3a. (F-I) Western blots and bar graphs showing relative APP expression (DIV7 4h after Wnt treatment) (G) and relative mRNA expression of APP (normalized with actin) (H) in cells treated with PBS/BSA or Wnt3a. (I) Western blots showing relative APP expression (DIV7 4h after Wnt treatment) in control (Ctrl) cells treated with PBS/BSA or Wnt3a. (J) Western blots showing relative APP expression (DIV7 4h after Wnt treatment) in cells treated with PBS/BSA or Wnt3a in the presence of the Wnt inhibitor Ly294002 (10uM). (K-L) Bar graphs showing relative APP expression (DIV7 4h after Wnt treatment) in cells treated with PBS/BSA or Wnt3a (K) and in cells treated with PBS/BSA or Wnt3a in the presence of the Wnt inhibitor Ly294002 (10uM) (L). (M-O) Western blots and bar graphs showing relative APP expression (DIV7 4h after Wnt treatment) (N) and relative mRNA expression of APP (normalized with actin) (O) in cells treated with PBS/BSA or Wnt3a+Wnt5a (M). (N) Bar graph showing relative APP expression (DIV7 4h after Wnt treatment) in cells treated with PBS/BSA or Wnt3a+Wnt5a. (O) Bar graph showing relative mRNA expression of APP (normalized with actin) in cells treated with APP-/- (ctrl), PBS/BSA, or Wnt3a+Wnt5a.

Figure 4 continued

down Wnt3a even with higher protein levels compared to wild type mAPP in the input. (B) mAPP localization after 4 hr PBS/BSA or Wnt3a treatment. Immunofluorescence for APP (red), Rab5 (green), Golgin97 (green), and Lamp1 (green) revealed mAPP localization in different intracellular compartments. The inset showed zoomed in images of the area in the white box and arrows indicated the overlap of mAPP with respective cellular compartment markers. Scale bar = 10 μ m. (C–E) Quantification of the overlap of mAPP with early endosome (C), TGN (D) or lysosome (E), respectively, after Wnt3a treatment. (n=33–54 cells, t-test). (F) Western blots of mAPP and Actin on the lysates of DIV7 primary cultured cortical neurons showed that mAPP protein expression level was altered after Wnt3a treatment. (G) Quantification of the western blots results for figure F. (n=three biological independent repeat, t-test). (H) qPCR results showed that mApp mRNA expression was not affected after Wnt3a treatment on DIV7. App^{-/-} mice derived primary neurons were used as a negative control. (n=three biological independent repeat, one-way ANOVA). (I and J) Western blots for APP showed that the Retromer inhibitor Ly294002 (J) could rescue Wnt3a-induced mAPP increase compared with control groups (I). (K and L) Quantification of the western blots results for figure I and J. (n=three biological independent repeat, t-test). (M) Western blots for mAPP expression 4 hr after Wnt3a and Wnt5a treatment at the same time on DIV7. PBS/BSA group acted as control group. (N) Quantification of the western blots results for figure M. (n=three biological independent repeat, t-test). (O) qPCR results for mApp mRNA expression in mApp knockout neurons (negative control), PBS/BSA treated control group neurons and Wnt3a+Wnt5a-treated group neurons. (n=three biological independent repeat, one-way ANOVA). Bars represent the mean \pm S.E.M. Samples collected from at least two independent experiments. *p<0.05, **p<0.01.

The online version of this article includes the following source data and figure supplement(s) for figure 4:

Source data 1. Co-immunoprecipitation (co-IP) of Wnt3a-V5 with full-length proteins mAPP-flag or mAPPL Δ CRD.

Source data 2. Western blots for mAPP and Actin after Wnt3a treatment on DIV7 primary cortical neurons.

Source data 3. Western blots for mAPP and Actin after Wnt3a treatment on DIV7 primary cortical neurons.

Source data 4. Western blots for mAPP and Actin after adding Ly294002 followed by Wnt3a treatment on DIV7 primary cortical neurons.

Source data 5. Western blots for mAPP and Actin after Wnt3a + Wnt5a treatment on DIV7 primary cortical neurons.

Figure supplement 1. APP affects beta-catenin expression after Wnt3a treatment.

Figure supplement 1—source data 1. Western blots for β -Catenin and Actin for APP-WT primary cultured cortical neurons after 4 hr of Wnt3a/5a treatment on DIV7 primary cortical neurons.

Figure supplement 1—source data 2. Western blots for β -Catenin and Actin for APP-KO primary cultured cortical neurons after 4 hr of Wnt3a/5a treatment on DIV7 primary cortical neurons.

Figure supplement 2. A β detection after Wnts treatment on DIV7 primary cortical neurons.

confirm this, we used Bafilomycin-A in combination with Wnt5a treatment. Bafilomycin-A treatment was performed 1 hr after Wnt5a addition as Wnt5a treatment already affected APP levels after 2 hr (**Figure 3—figure supplement 5**) to inhibit the lysosome and found that this restored mAPP to control levels (**Figure 3I–L**). These data suggest that non-canonical Wnt5a-PCP signaling reduces mAPP stability.

Wnt3a binds to and stabilizes APP via the CRD

We wondered whether mAPP can also bind other members of the Wnt family of ligands. Wnt3a is one of the 19 Wnt members in mouse and human. During development, Wnt3a usually induces β -catenin signaling pathway which plays an important role in gene expression, cell proliferation, and differentiation (**Mulligan and Cheyette, 2012; Rosso and Inestrosa, 2013**). Recent studies suggest that Wnt3a and beta-Catenin signaling may be involved in AD pathology (**Parr et al., 2015; Tapia-Rojas et al., 2016**). More interestingly, studies on mouse AD models showed that Wnt3a and Wnt5a interact competitively and antagonistically with regard to APP-mediated synapse loss (**Sellers et al., 2018; Elliott et al., 2018**). We therefore wondered whether, like Wnt5a, Wnt3a also binds to mAPP through the conserved CRD and regulates its levels. To test this, we performed IP experiments with Wnt3a. We found that fl-mAPP and Wnt3a co-IP in a CRD-dependent fashion (**Figure 4A**). We next tested the effects of Wnt3a treatment on APP trafficking. As shown in and **Figure 3—figure supplement 2(A)**, The fraction of mAPP co-localized with early endosomes (**Figure 4B,C**) and recycling endosome (**Figure 3—figure supplement 2A,D**) was not affected after 2 hr and 4 hr of Wnt3a treatment. However, more mAPP was present in the TGN, with no effect on the lysosomal mAPP fraction after 2 hr (**Figure 3—figure supplement 2D,G**) and 4 hr (**Figure 4B–E**) of Wnt3a treatment. The expression levels of Rab5, Golgin97 and Lamp1 were not affected after Wnt3a treatment (**Figure 3—figure supplement 4**). Western blot analysis showed increased fl-mAPP upon Wnt3a treatment (**Figure 4F,G**), but no effect on mRNA levels (**Figure 4H**). There is evidence that mAPP is recycled back to the TGN from early endosomes through the retrograde pathway (**Vagnozzi and Praticò, 2019**). To test whether Wnt3a regulates mAPP retro trafficking to the TGN, we co-treated primary neurons with Wnt3a and a retromer inhibitor (LY294002), retromer inhibitor treatment was

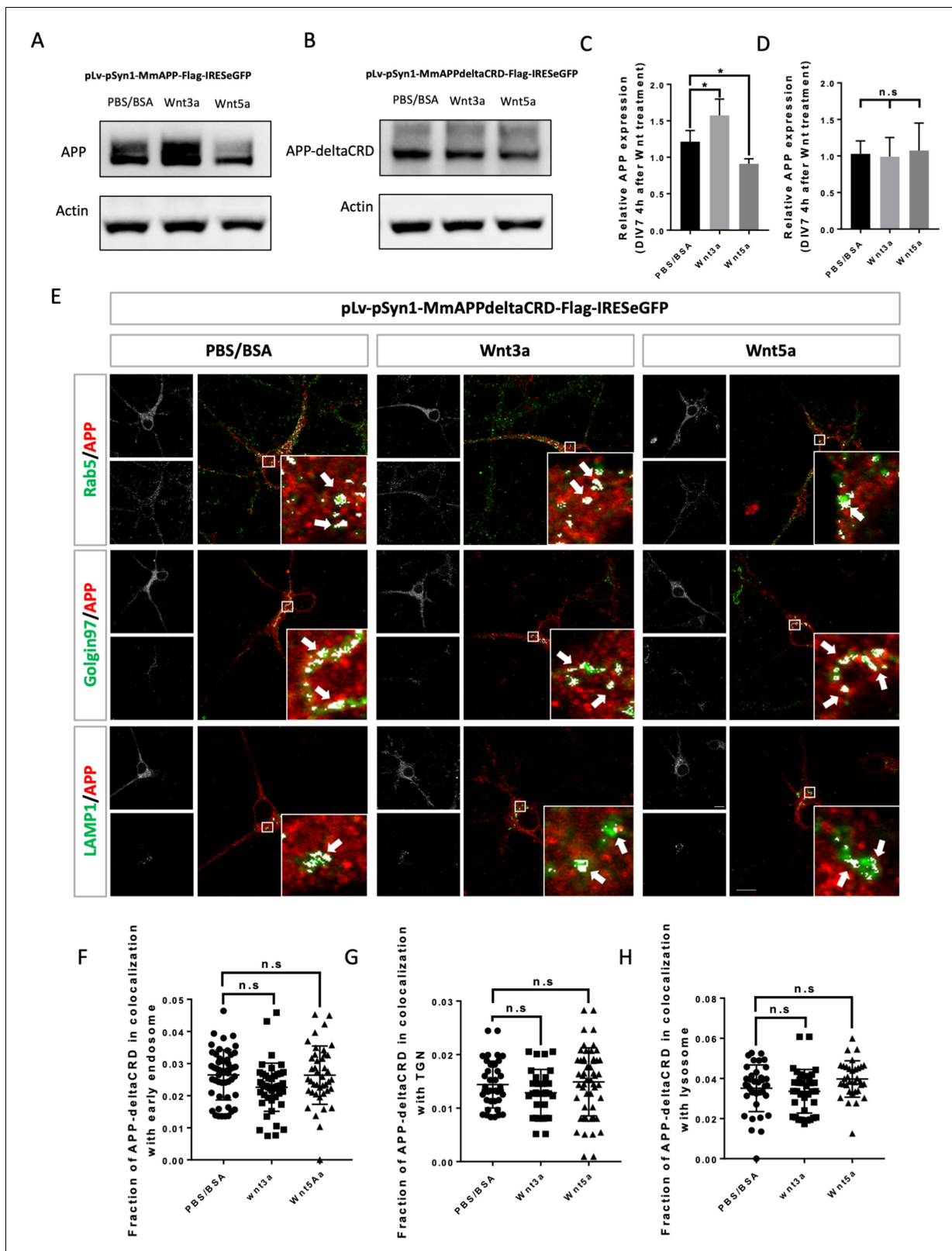


Figure 5. CRD is required for Wnt3a/5a to affect APP trafficking and expression. (A and B) Western blots for the detection of exogenous APP expression 4 hr after PBS/BSA (control), Wnt3a or Wnt5a treatment at DIV7 in APP-KO primary cultured neurons which were transfected with pLv-pSyn1-mAPP-Flag-IRESeGFP (A) or pLv-pSyn1-mAPP Δ CRD-Flag-IRESeGFP (B) lenti-virus. (C and D) Quantification of the western blots results for figure A and B, respectively. (n=three biological independent repeat, one-way ANOVA). (E) Localization of exogenous mAPP expression in APP-KO primary cultured neurons. (F-H) Quantification of APP-deltaCRD colocalization with early endosome (F), TGN (G) and lysosome (H). (n=three biological independent repeat, one-way ANOVA). Figure 5 continued on next page

Figure 5 continued

cortical neurons 4 hr after Wnt3a or Wnt5a treatment. Immunofluorescence for APP (red), Rab5 (green), Golgin97 (green), and Lamp1 (green) revealed mAPP localization in different intracellular compartments. The inset showed zoomed in images of the area in the white box and arrows indicated the overlap of mAPP with respective cellular compartment markers. (F–H) Quantification of the overlap of mAPP with early endosome (F), TGN (G), or lysosome (H), respectively, after Wnt3a or Wnt5a treatment. (n=32–51 cells, one-way ANOVA). Bars represent the mean \pm S.E.M. Samples collected from at least two independent experiments. *p<0.05.

The online version of this article includes the following source data and figure supplement(s) for figure 5:

- Source data 1.** Western blots for APP and Actin after lenti-virus transduction followed by Wnt3a or Wnt5a treatment on DIV7 primary cortical neurons.
- Source data 2.** Western blots for APP-deltaCRD and Actin after lenti-virus transduction followed by Wnt3a or Wnt5a treatment on DIV7 primary cortical neurons.
- Figure supplement 1.** Lenti-virus-induced exogenous mAPP expressed in mAPP knock out primary cortical neuron.
- Figure supplement 1—source data 1.** Western blots for flag and Actin after lenti-virus transduction on DIV7 primary cortical neurons.
- Figure supplement 1—source data 2.** Western blots for APP and Actin after lenti-virus transduction on DIV7 primary cortical neurons.
- Figure supplement 2.** Lenti-virus induced exogenous interact with Wnts in mAPP knock out primary cortical neuron.

performed 1 hr after Wnt3a addition as Wnt3a treatment could affected APP protein expression clearly 2 hr later (**Figure 3—figure supplement 5**). This reversed the effect of Wnt3a on mAPP trafficking protein levels (**Figure 4I–L**). Then, we tested the effects of simultaneous treatment with Wnt3a and Wnt5a. This resulted in no change to APP protein levels compared to controls, suggesting that Wnt3a and Wnt5a neutralize each other's effects on mAPP (**Figure 4M,N**), again with no effects on mRNA levels (**Figure 4O**). We and others have previously shown that APP is a key component in both Wnt canonical and non-canonical Wnt signaling (**Elliott et al., 2018; Soldano et al., 2013**). We confirmed this in our system and found that treatment with Wnt3a resulted in β -catenin accumulation in APP-WT, but not APP-KO, primary cortical neurons at DIV7 (**Figure 4—figure supplement 1A–D**). We also observed a tendency toward a decrease in β -catenin upon Wnt5a treatment, but this did not reach statistical significance.

Because Wnt treatment affects APP trafficking and expression, we tested A β 40 and A β 42 production in primary cortical neurons at DIV7 after 4 hr treatment of with Wnt3a or Wnt5a. Our data show that a 4 hr Wnt3a/5a treatment has a long-lasting effect on A β 40/42 production and that those effects are antagonistic. Consistent with Wnt3a favoring recycling of APP, we found that Wnt3a treatment significantly decrease A β 40/42 production (**Figure 4—figure supplement 2A,B**). In contrast, Wnt5a treatment, which induces APP internalization into acidic compartments, resulted in an increase in A β 40/42 production (**Figure 4—figure supplement 2C,D**). Importantly, these data are in accordance with other reports that Wnt/catenin pathway favors non-amyloidogenic APP processing while Wnt/PCP signaling does the opposite (**Elliott et al., 2018**).

Taken together, these data indicate that Wnt3a also binds to mAPP via the CRD and regulates mAPP trafficking and expression and that Wnt5a and Wnt3a act antagonistically to regulate APP protein homeostasis.

The CRD is required for Wnt-mediated regulation of APP trafficking and expression

Our data thus far show that APP interacts with Wnts through its CRD and that Wnts regulate APP intracellular trafficking and expression. We therefore asked whether the CRD is required for the effects of Wnts on mAPP. To address this question, we created two lentiviral vectors: pLv-pSyn1-mAPP-Flag-IRES-eGFP (flag-tagged fl-mAPP) and pLv-pSyn1-mAPP Δ CRD-Flag-IRES-eGFP (flag-tagged mAPP Δ CRD). Primary cortical neurons from *App* knockout mice were transduced with the fl-mAPP or mAPP Δ CRD vectors, or a control GFP vector (pLv-pSyn1-IRES-eGFP) exogenous APP/APP Δ CRD was detectable using either anti-APP or anti-flag antibodies (**Figure 5—figure supplement 1A–C**). In neurons transduced with wild-type mAPP, we confirmed that mAPP expression could be increased and decreased by Wnt3a and Wnt5a treatments, respectively (**Figure 5A,C**). In contrast, in neurons transduced with mAPP Δ CRD those effects were eliminated (**Figure 5B,D**). Finally, we performed IF to trace mAPP and mAPP Δ CRD localization. Neurons transduced with wild type mAPP showed the same results as wild-type neurons with more mAPP in the TGN upon 4 hr of Wnt3a treatment and more mAPP in lysosomes upon 2 hr (**Figure 3—figure supplement 2B,E,H**) and 4 hr of Wnt5a treatment (**Figure 5—figure supplement 2A–D**). Similarly, there was no effect on

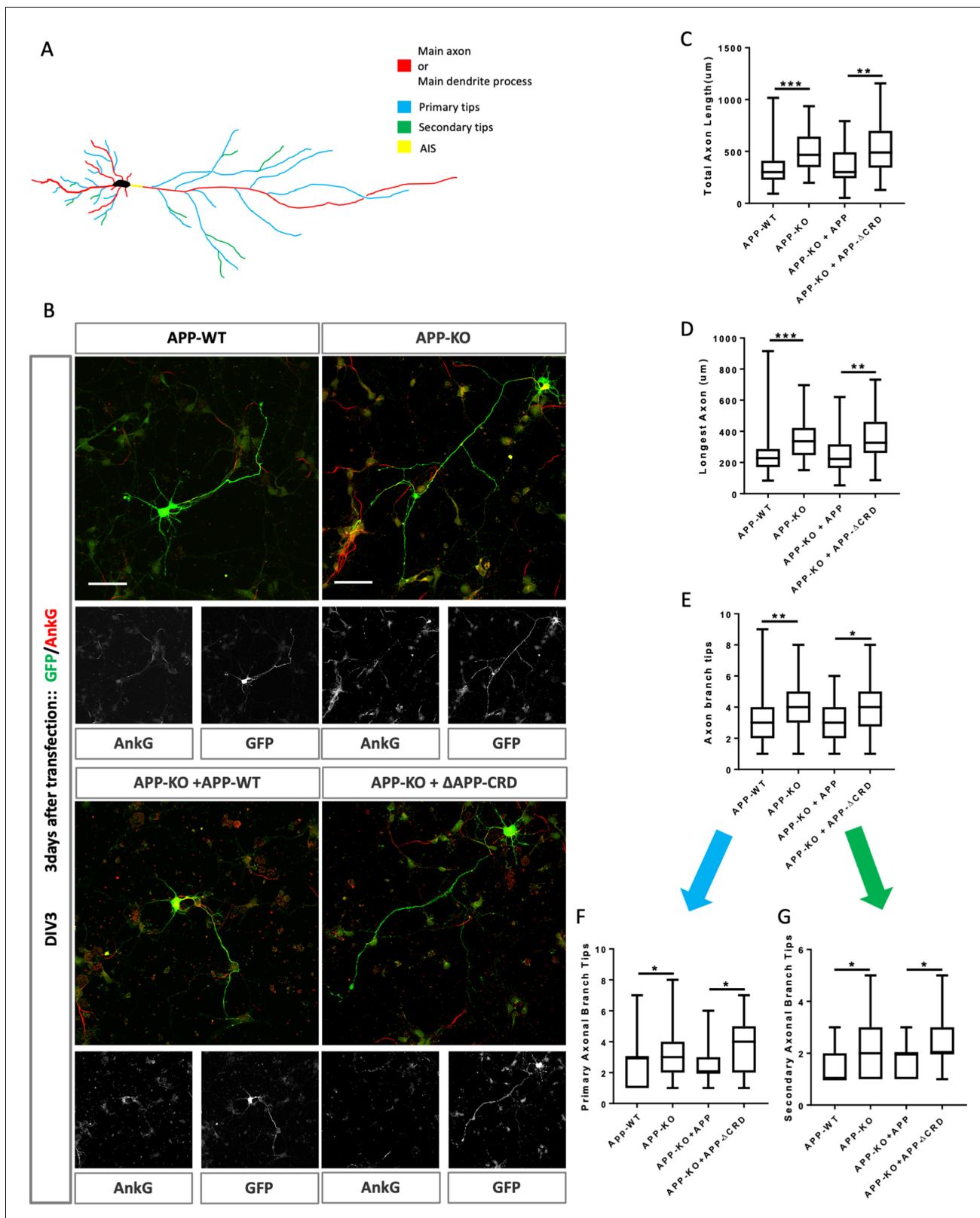


Figure 6. Cysteine-Rich Domain is critical for APP to regulate neurite outgrowth at DIV3. (A) Schematic of a primary neuron. Colored lines indicate axonal or dendritic branch tips which were quantified. Yellow indicates the Axon Initial Segment (AIS) marked with Ankyrin G in experiments. (B) Representative confocal images for GFP (green) and Ankyrin G (red) immunostaining at DIV3 on primary cultured cortical neurons of the four genotypes examined: mAPP wild type, mAPP-KO, and mAPP-KO rescued with mAPP or CRD-mutant mAPP. Transfected plasmids containing GFP alone, mAPP-
Figure 6 continued on next page

Figure 6 continued

flag-GFP or mAPP Δ CRD-flag-GFP, which was performed at the onset of cell seeding. Scale bar = 50 μ m. (C–E). Quantification of three parameters on these four genotypes at DIV3: the total axon length (the main axonal process and the branches deriving from the main process, C), the longest axonal length (D), the total axonal branch tips (E), primary branch tips (F) and secondary branch tips (G). (n=59–70 cells, one-way ANOVA). Bars represent the mean \pm S.E.M. Samples collected from at least two independent experiments. *p<0.05, **p<0.01 ***p<0.001.

The online version of this article includes the following figure supplement(s) for figure 6:

Figure supplement 1. Neurite outgrowth is unaffected in APP knock out neurons at DIV2.

Figure supplement 2. Analysis of dendritic outgrowth and axon complexity index at DIV3.

colocalization with recycling endosome upon 2 or 4 hr of treatment (**Figure 3—figure supplement 3, E**). All these effects were abolished in neurons transduced with mAPP Δ CRD (**Figure 5E–H; Figure 3—figure supplement 3F; Figure 3—figure supplement 2C,F,I**).

In summary, these data show that the CRD of mAPP is critical for Wnt3a/5a binding and mediates the effects of Wnts on mAPP trafficking and expression.

CRD is critical for APP to regulate neurite outgrowth and complexity

APP and its proteolytic products have been reported to affect neurite outgrowth during development (**Billnitzer et al., 2013; Young-Pearse et al., 2008**) in different systems. We used primary cortical neuron derived from E16.5 mice embryos to investigate if the CRD of mAPP is required for regulation of neurite outgrowth by mAPP. We examined axonal and dendritic outgrowth (**Figure 6A**) at three developmental stages in vitro: DIV2, DIV3, and DIV7 (**Dotti et al., 1988**).

While we found no effect on initial outgrowth at DIV2 (**Figure 6—figure supplement 1A–F**), at DIV3 mAPP knockout neurons exhibit increased axonal outgrowth compared to controls reflected in three parameters: total axon length, longest axon length, and the number of branch tips (**Figure 6B–E**). In contrast, dendritic outgrowth was not different from controls (**Figure 6—figure supplement 2A–C**). We asked whether the CRD was required for mAPP function during neurite outgrowth. To this end, we transfected mAPP knockout neurons with either fl-mAPP or mAPP Δ CRD. Increased axonal length and axonal branch tips were rescued by the fl-mAPP but not by the form lacking the CRD at DIV3 (**Figure 6B–E**). Next, we analyzed axonal branching in greater detail and found that loss of mAPP increased the numbers of both primary and secondary axonal branches at DIV3, an increase that was rescued by fl-mAPP but not by mAPP Δ CRD (**Figure 6F,G**). Finally, we examined the Axon Complexity Index (ACI) (**Wong et al., 2017**), which measures the ratio of branches of different orders to total branch number, at DIV3. At this early stage, the ACI showed a tendency to increase in mAPP knockout neurons that was not significant (**Figure 6—figure supplement 2D**), likely because both primary and secondary branches show a similar level of increase. Together these data suggest an overall increase in axonal growth. In contrast to axonal growth, we found no significant alterations in dendritic length or branching (**Figure 6—figure supplement 2E–G**) consistent with the fact that the spur in dendritic outgrowth is largely initiated at DIV4 (**Polleux and Snider, 2010; Barnes and Polleux, 2009**).

To further analyze neurite outgrowth, we examined axonal and dendritic growth at DIV7. By this stage, mAPP knockout neurons showed an increased ACI (**Figure 7A,B**). In contrast, total axonal length, longest axon length, and the total number of branch tips was not significantly different (**Figure 7C–E**). The increase in axonal complexity in mAPP knockout neurons was due to a significant reduction in the number of primary branches and a significant increase in the number of secondary branches (**Figure 7F,G**). Once again, all phenotypes were rescued by fl-mAPP but not mAPP Δ CRD.

Finally, we examined dendritic growth at DIV7. We observed no difference in total dendrite length or the size of the longest dendrite (**Figure 7—figure supplement 1A,B**), but observed a significant decrease in the total number of dendritic processes in mAPP knockout neurons compared to controls (**Figure 7—figure supplement 1C**). This reduction was due to the presence of fewer main dendritic processes in mAPP knockout neurons but no effect was observed on the primary or secondary dendritic branches (**Figure 7—figure supplement 1D–F**). All phenotypes were rescued by fl-mAPP but not mAPP Δ CRD. Taken together, our results show that the role of APP in neuronal maturation requires the CRD domain.

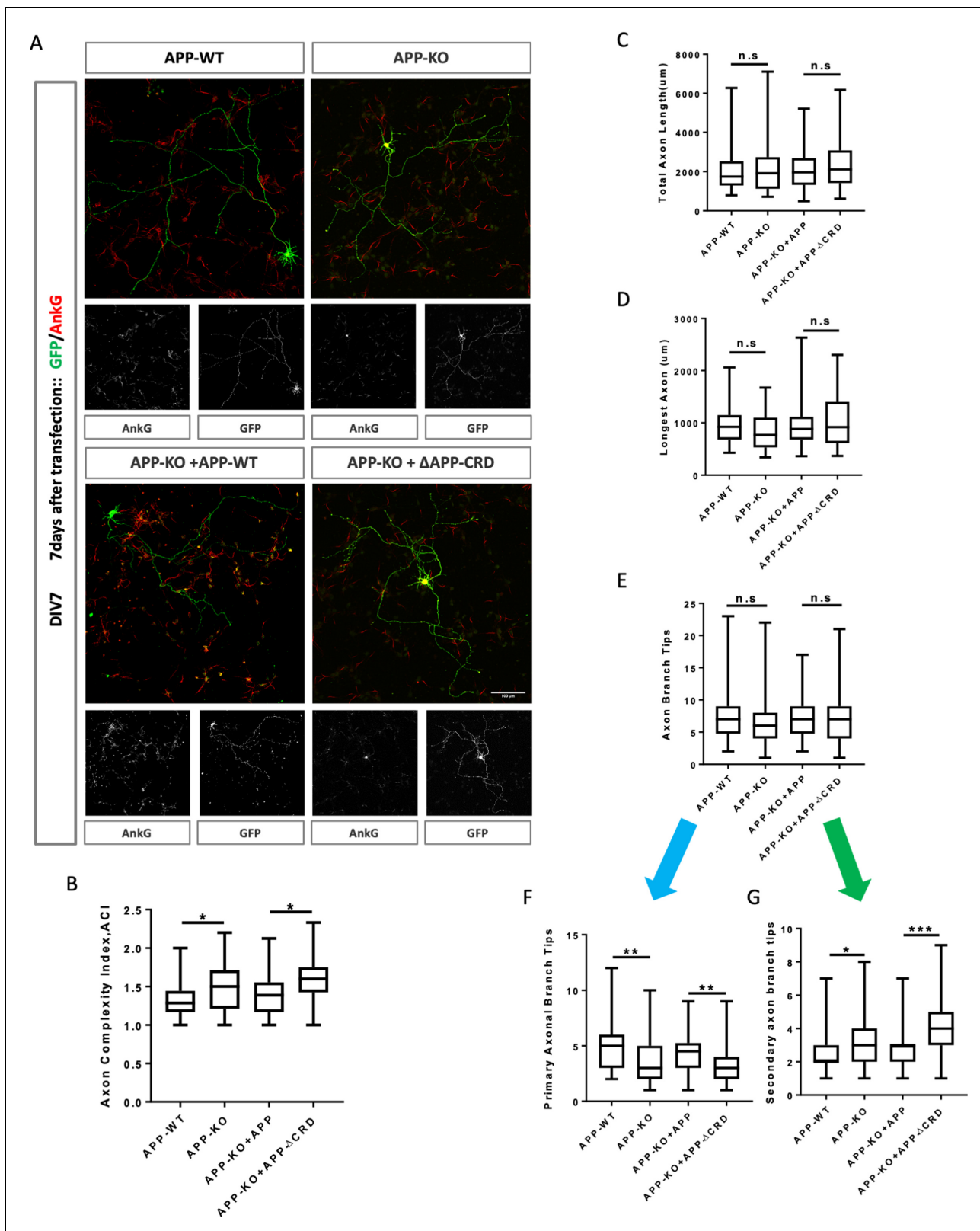


Figure 7. Cysteine-Rich Domain is critical for APP to regulate neurite outgrowth and complexity at DIV7. (A) Representative confocal images for GFP (green) and AnkG (red) immunostaining at DIV7 on primary cultured cortical neurons of the four genotypes examined: mAPP wild type, mAPP- KO and mAPP-KO rescued with APP or CRD-mutant APP. Transfected plasmids containing GFP alone, mAPP-flag-GFP or mAPPΔCRD-flag-GFP, which was performed at the onset of cell seeding. Scale bar = 100 um. (B–G) Analysis of Axon complexity Index (ACI, B), the total axonal length (C), the longest axon (D), the number of axon branch tips (E), the number of primary axonal branch tips (F) and the number of secondary axon branch tips (G) for each genotype. *Figure 7 continued on next page*

Figure 7 continued

axonal length (D), all axonal branch tips (E), the primary branch tips (F) and the secondary branch tips (G) at DIV7. (n=54 cells, one-way ANOVA). Bars represent the mean \pm S.E.M. Samples collected from at least two independent experiments. *p<0.05, **p<0.01, ***p<0.001.

The online version of this article includes the following figure supplement(s) for figure 7:

Figure supplement 1. Outgrowth and complexity analysis of neurite at DIV7.

Wnts regulate neurite development in a CRD dependent manner

The Wnt pathway plays an important role in regulating neurite development, therefore we tested if the APP CRD is important for the interaction between APP and Wnt in regulating neurite outgrowth. To address this question, we analyzed neurite outgrowth in APP-KO primary cortical neurons rescued with APP-WT or APP- Δ CRD plasmids after Wnt3a/5a treatment. On DIV3 Wnt3a treatment significantly increased total axon length, the length of longest axon and axon branch tips in the presence of fl-APP but not APP- Δ CRD (Figure 8A,B,C). These data suggest that APP mediates Wnt3a effects on axonal outgrowth. In contrast to Wnt3a, Wnt5a treatment had no effect in the presence of fl-APP but resulted in increased axonal length when the CRD domain was removed. These data show that APP normally protects axons from the effects of Wnt5a at this developmental stage and that the CRD is required for this (Figure 8B). Thus, APP promotes Wnt3a and antagonizes Wnt5a effects on neurons at DIV3 via the CRD domain. Similarly, on DIV7 we found a positive Wnt3a effect on axon complexity which was observed in the presence of fl-APP but not APP- Δ CRD (Figure 8D). In contrast Wnt5a had no effect. Finally, we found that treatment with either Wnt3a or Wnt5a decreases the number of the main dendrites in the presence of fl-APP and the effect is absent or even reversed in the presence of APP- Δ CRD (Figure 8E). Together, these data show that the CRD of APP is required for Wnt3a/5a to regulate neurite outgrowth in cortical primary neurons.

Discussion

Here, we identify a previously unknown conserved Wnt receptor function for APP proteins. We show that APP binds both canonical and non-canonical Wnt ligands via a conserved CRD and that this binding regulates the levels of full-length APP by regulating its intracellular trafficking from early endosomes to the trans Golgi network versus the lysosome. Finally, we show that APP through the CRD regulates neurite growth and axon branching complexity in primary mouse cortical neurons.

A function for APP as a cell surface receptor has been proposed for quite a long time (Kang et al., 1987). The first strong evidence came from the structure of APP which shares similarity with type I transmembrane receptors. For example the growth factor like domain (GFLD) in the E1 region of APP could act as a ligand-binding site, and disulfide bridges within the same E1 area could further facilitate ligand-induced signal transduction by stabilizing the structure of APP ectodomain (Reinhard et al., 2005; Rossjohn et al., 1999; Stahl et al., 2014; Kaden et al., 2009). In addition, the site-specific proteolytic processing property of APP resembles several membrane receptors and constitute a second line of evidence. For instance, both APP and Notch are processed by γ -secretase and release the intracellular domain AICD and NICD, respectively, to induce transcriptional activity by nuclear transfer of the ICDs (Chang et al., 2006; Ables et al., 2011). Several putative ligands have been proposed including proteolytic products of APP itself. Interestingly, a conserved CRD within the E1 region of APP makes APP a putative Wnt receptor as the CRD is required for the binding between Wnt and its receptor and co-receptor like Frizzled Ror-2 and Musk (Niehrs, 2012), although the crystal structure of the APP CRD is different from that of classic Wnt receptors. In this study, using immunoprecipitation we have shown that mouse APP binds in a CRD-dependent manner to Wnt3a and Wnt5a the two well-known ligands for triggering canonical or non-canonical Wnt signaling pathways, respectively. Based on these data, we speculate that APP might act as a conserved Wnt receptor as its CRD is highly conserved across species, and that the binding may not be limited to Wnt3a or Wnt5a, but also apply to all other Wnt family members. As Wnt signaling is critical for development and tissue homeostasis, the role of APP as a component or putative receptor or co-receptor in Wnt signaling should be carefully studied. The difficulty to explore the exact role of APP may not only come from the complexity of Wnt signaling, but also from the structural properties of APP itself. For example, the extracellular domain of APP harbors several binding site for the

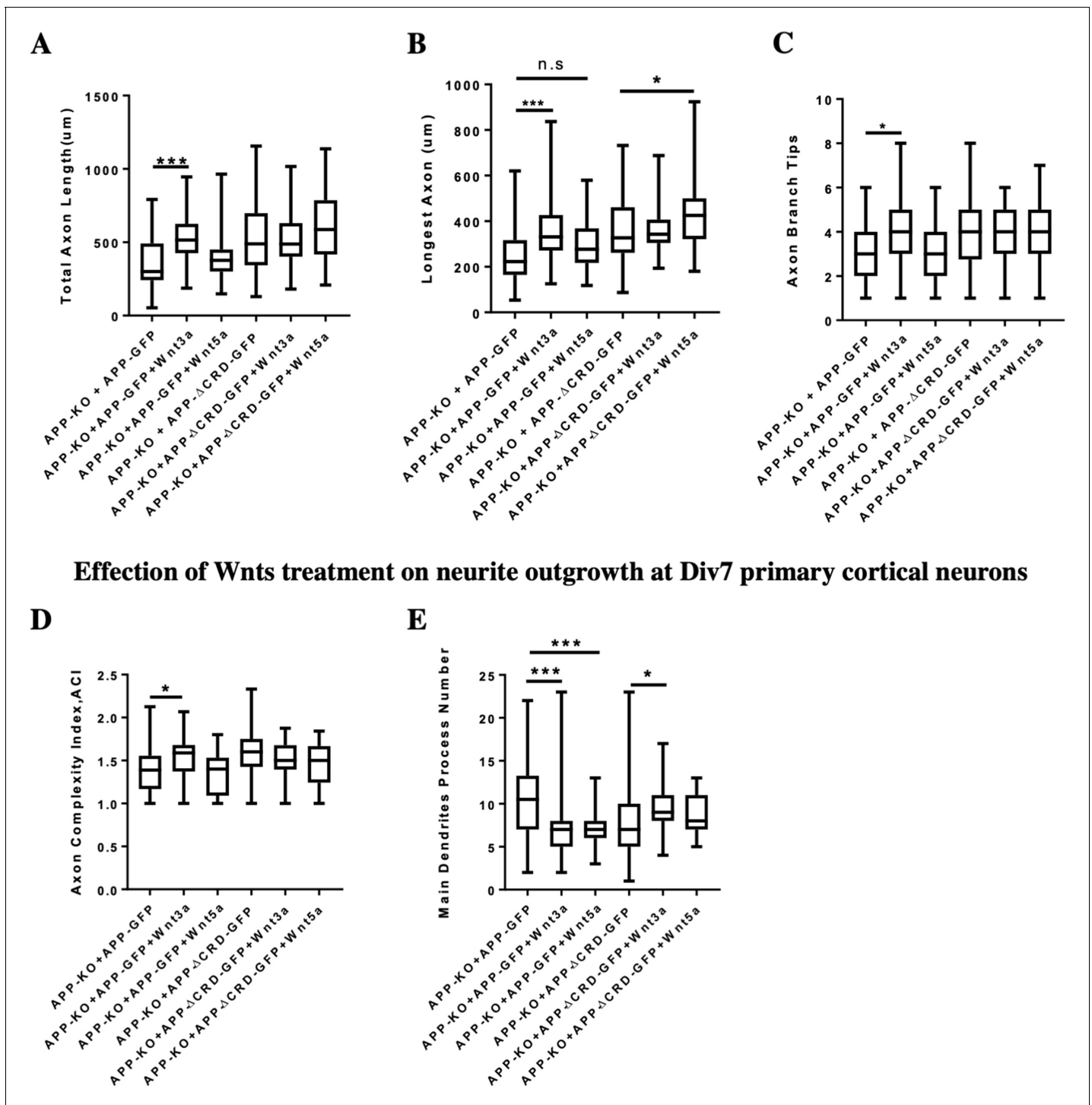


Figure 8. Neurite outgrowth analysis at DIV3 and DIV7 after Wnts treatment. (A–C) Quantification of total axon length (A), the longest axon length (B), and axon branch tips (C) from DIV3 cultured APP-KO primary cortical neuron after Wnts treatment rescued with APP-WT or APP- Δ CRD, respectively. (n=46–63 cells, one-way ANOVA). (D and E) Analysis of axon complexity (D) and the main dendritic process number (E) from DIV7 cultured APP-KO primary cortical neuron after Wnts treatment rescued with APP-WT or APP- Δ CRD, respectively. (n=47–54 cells, one-way ANOVA). Bars represent the mean \pm S.E.M. Samples collected from at least two independent experiments. *P<0.05, ***p<0.001.

molecules in the extracellular matrix (ECM), such as the Heparin binding domain (HBD) is not only exist in E1 area a second HBD has been found in the E2 region (Deys *et al.*, 2016). A recent study has shown that LRP6, the co-receptor of canonical Wnt signaling, could directly bind to APP

(Elliott et al., 2018). Using peptide Mapping array this group further revealed several binding sites (20–70 amino acids in length) in the ectodomain of APP, and one of the sites (34 amino acids) is located within the APP CRD. Based on our IP results indicating a Wnt receptor function for APP, an obvious question arises as to whether LRP6 and APP compete for Wnt. Before trying to address this problem, several issues need to be resolved. First, as in our IP experiments the whole CRD (150 amino acids) was deleted it is not clear if specific sequences inside the CRD are critical for Wnt binding that may or may not overlap with the reported LRP6-binding site. A second important point is that the results of the peptide mapping array may not reflect the exact binding site for LRP6 as these short synthesized peptides may lack information embedded in the 3D structure like the disulfide bridges formed by Cysteines that may be critical for maintaining the stability of the APP extracellular domain (Rossjohn et al., 1999; Stahl et al., 2014). Significant further biophysical and biochemical analysis is required to understand the details of the interaction and various components of the Wnt receptor complex.

APP has been extensively reported to be involved in regulating neurite outgrowth (Billnitzer et al., 2013; Young-Pearse et al., 2008; Araki et al., 1991; Southam et al., 2019; Small et al., 1994; Perez et al., 1997), with conflicting conclusions as to whether APP promotes or inhibits neurite outgrowth. In our experiments, we found that while in *Drosophila* APPL loss reduced axonal growth, the comparison of axonal outgrowth and branching in primary cortical neuron derived from mAPP wild type or mAPP knock out mice at DIV2, DIV3 and DIV7 showed that loss of mAPP significantly accelerated axonal maturation. Specifically, we found that the initial phase of axonal growth at DIV2 is unaffected, but that APP mutant axons grow longer at DIV3 and then show increased axon complexity at DIV7. We therefore suggest that the conflicting data in the literature may arise from examining different types of neurons at different time points, where the requirement of APP may differ in a context-specific manner. We speculate that this context specificity may in part be due to the levels and types of Wnt ligands present in the environment.

Finally, our findings suggest that in addition to the well-described proteolytic processing of APP, the regulation of its recycling by Wnt ligands may be crucial for its function. It is important to note that, like proteolytic processing, Wnt ligands regulate APP stability post-translationally, as we found no effect on *App* mRNA levels upon Wnt treatment. With regard to the role of APP processing in Alzheimer's disease, recently published work suggests that an imbalance between Wnt3a/canonical signaling pathway and the Wnt5a/PCP signaling pathway at the initial step of amyloid beta production could trigger a vicious cycle favoring the amyloidogenic processing of APP (Sellers et al., 2018; Elliott et al., 2018). Our findings that Wnt3a and Wnt5a have opposite effects on amyloid beta production provide a mechanistic framework for understanding how the normal physiological function of APP directly impacts the generation of a key marker of AD, and thus potentially links the normal activity of APP to its role in neurodegeneration. Whether and how the modulation of APP's role in Wnt signaling may offer future therapeutic avenues for AD is an exciting venue for future research.

Materials and methods

Key resources table

Reagent type (species) or resource	Designation	Source or reference	Identifiers	Additional information
Antibody	Mouse monoclonal anti-FasII (1D4)	Developmental Studies Hybridoma Bank (DSHB)	AB_528235 RRID:AB_528235	IF (1:50)
Antibody	Rabbit polyclonal anti-Wnt5a	Cell Signaling	Cat# 2392 RRID:AB_2304419	WB (1:1000)
Antibody	Rabbit polyclonal anti-GFP	Invitrogen	Cat# A-11122, RRID:AB_221569	IF (1:500)
Antibody	Rabbit polyclonal anti-APP	Synaptic Systems	Cat# 127 003 RRID:AB_2056967	IF (1:100) WB (1:1000)
Antibody	Mouse monoclonal anti-rab5	Synaptic Systems	Cat# 108 011 RRID:AB_887773	IF (1:100) WB (1:1000)

Continued on next page

Continued

Reagent type (species) or resource	Designation	Source or reference	Identifiers	Additional information
Antibody	Mouse monoclonal anti-rab11a	Santa Cruz	Cat# sc-166523, RRID:AB_2173466	IF (1:20)
Antibody	Mouse monoclonal anti- Golgin-97	Invitrogen	Cat# A-21270, RRID:AB_221447	IF (1:100) WB (1:1000)
Antibody	Rat monoclonal anti-Lamp1	Santa Cruz	Cat# sc-19992, RRID:AB_2134495	IF (1:20) WB (1:200)
Antibody	Chicken polyclonal anti-GFP	Abcam	Cat# ab13970, RRID:AB_300798	IF (1:200)
Antibody	Guinea pig Polyclonal antiserum anti-Ankyrin G	Synaptic Systems	Cat# 386004 RRID:AB_2725774	IF (1:100)
Antibody	Rabbit Polyclonal Anti-V5	Millipore	Cat# AB3792 RRID:AB_91591	IP (1:20) WB (1:1000)
Antibody	Rat Monoclonal Anti-DYKDDDDK Epitope Tag	Novus	Cat# NBP1-06712 RRID:AB_1625981	IP (1:20) WB (1:1000)
Antibody	Mouse Monoclonal Anti-c-Myc	Sigma-Aldrich	Cat# M4439 RRID:AB_439694	IP (1:20) WB (1:1000)
Antibody	Goat anti-Chicken IgY (H+L), Alexa Fluor488	Invitrogen	Cat# A-11039, RRID:AB_142924	IF (1:500)
Antibody	Goat anti-Rabbit IgG (H+L), Alexa Fluor488	Invitrogen	Cat# A-11008, RRID:AB_143165	IF (1:500)
Antibody	Goat anti-Rat IgG (H+L), Alexa Fluor488	Invitrogen	Cat# A-11006, RRID:AB_141373	IF (1:500)
Antibody	Goat anti- Mouse IgG (H+L), Alexa Fluor488	Invitrogen	Cat# A-11029, RRID:AB_138404	IF (1:500)
Antibody	Goat anti-Rabbit IgG (H+L), Alexa Fluor555	Invitrogen	Cat# A-11034, RRID:AB_2576217	IF (1:500)
Antibody	Goat anti-Guinea Pig IgG (H+L), Alexa Fluor555	Invitrogen	Cat# A-21435, RRID:AB_2535856	IF (1:500)
Antibody	Peroxidase AffiniPure Donkey Anti-Mouse IgG (H+L)	Jackson Immuno Research Labs	Cat# 715-035-150, RRID:AB_2340770	WB (1:4000)
Antibody	Peroxidase AffiniPure Donkey Anti-Rabbit IgG (H+L)	Jackson Immuno Research Labs	Cat# 711-035-152, RRID:AB_10015282	WB (1:4000)
Antibody	Peroxidase AffiniPure Donkey Anti-Rat IgG (H+L)	Jackson Immuno Research Labs	Cat# 712-035-153, RRID:AB_2340639	WB (1:4000)
Chemical compound, drug	Triton X-100	Sigma	Cat#X100	In PBS 0.1%
Chemical compound, drug	Trizol Reagent	Invitrogen	Cat#15596026	
Chemical compound, drug	L15 medium	Gibco	11415064	Medium for embryo brain isolation on ice
Chemical compound, drug	Mounting Medium	Vector Laboratories	Cat#H-1000	
Chemical compound, drug	0.05% trypsin/EDTA	Gibco	25300-054	
Chemical compound, drug	SVF	Invitrogen	10270106	
Chemical compound, drug	DNase	Serlabo	LS002138	
Chemical compound, drug	Neurobasal medium	Gibco	21103049	
Chemical compound, drug	B27 supplement	Gibco	17504-044	

Continued on next page

Continued

Reagent type (species) or resource	Designation	Source or reference	Identifiers	Additional information
Chemical compound, drug	L-glutamax	Gibco	35050-061	
Chemical compound, drug	Wnt3a	R and D Systems	645-WN-010	
Chemical compound, drug	Wnt5a	R and D Systems	1324-WNP-010	
Chemical compound, drug	Bafilomycin A1	invitrogen	88899-55-2	
Chemical compound, drug	LY294002	Sigma	L9908	
Chemical compound, drug	Lipofectamine 3000	ThermoFisher	Cat#L3000008	
Chemical compound, drug	DMEM	Gibco	Cat#10566016	
Chemical compound, drug	Penicillin-Streptomycin	Gibco	Cat#15140122	
Biological sample (<i>M. musculus</i>)	APP-KO mouse	A gift from Bart De Strooper's lab	N/A	
Cell line (<i>Homo-sapiens</i>)	Hek293	A gift from Marie-Claude Potier's lab	N/A	
Sequence-based reagent	mAPP_F	This paper Ordered from IDT	PCR primers	CATCCAGAACTGGTGCAAGCG
Sequence-based reagent	mAPP_R	This paper Ordered from IDT	PCR primers	GACGGTGTGCCAGTGAAGATG
Sequence-based reagent	β -actin _F	This paper Ordered from IDT er	PCR primers	TCCATCATGAAGTGTGACGT
Sequence-based reagent	β -actin _R	This paper Ordered from IDT r	PCR primers	GAGCAATGATCTTGATCTTCAT
Transfected construct (<i>M. musculus</i>)	pLv-pSyn1-mAPP-Flag-IRES-eGFP	ICM-institute, Virus facility	N/A	Lentiviral construct to transfect and express the mAPP
Transfected construct (<i>M. musculus</i>)	pLv-pSyn1-mAPP Δ CRD-Flag-IRES-eGFP	ICM-institute, Virus facility	N/A	Lentiviral construct to transfect and express the mAPP- Δ CRD
Transfected construct (<i>M. musculus</i>)	pLv-pSyn1- eGFP	ICM-institute, Virus facility	N/A	Lentiviral construct to transfect and express the GFP
Transfected construct (<i>M. musculus</i>)	pCDNA3-mApp-FLAG-IRES-eGFP	This paper	N/A	transfected construct
Transfected construct (<i>M. musculus</i>)	pCDNA3-mAPP Δ CRD-FLAG-IRES-eGFP	This paper	N/A	transfected construct
Transfected construct (<i>M. musculus</i>)	pCDNA3-Wnt5a-myc	This paper	N/A	transfected construct
Transfected construct (<i>M. musculus</i>)	pCDNA-Wnt3A-V5	This paper	N/A	transfected construct
Transfected construct (human)	pCDNA3-hApp-FLAG-IRES-eGFP	This paper	N/A	transfected construct
Transfected construct (human)	pCDNA3-hAPP Δ CRD-FLAG-IRES-eGFP	This paper	N/A	transfected construct
Commercial assay or kit	QuantiTect Reverse Transcription Kit	Qiagen	Cat# 205311	
Commercial assay or kit	LightCycler480 SYBR Green I Master	Roche	Cat# 04707516001	
Commercial assay or kit	4–12% polyacrylamide gels (SDS-PAGE)	ThermoFisher	NW04122BOX	

Continued on next page

Continued

Reagent type (species) or resource	Designation	Source or reference	Identifiers	Additional information
Commercial assay or kit	Protein G sepharose beads	ThermoFisher	Ref.10612D Lot.00644644	
Other	Nikon	A1-R		
Other	Olympus	FV-1200		
Other	DAPI	Sigma	Cat# D9564	1 ug/ml
Software, algorithm	GraphPad Prism software	GraphPad Prism (https://graphpad.com)	RRID:SCR_015807	
Software, algorithm	ImageJ software	ImageJ (http://imagej.nih.gov/ij/)	RRID:SCR_003070	

Drosophila stocks and maintenance

Flies were raised at 25°C, on standard cornmeal and molasses medium. The stocks used in this study are: w*, Appl^d; Vang^{stbm-6}; w1118, Wnt5⁴⁰⁰; P247Gal4; w*, Appl^d, Wnt5⁴⁰⁰.

Cloning

All constructs were generated by PCR amplification and overlap extension PCR. PCR products were inserted into the respective vectors by classical restriction enzyme cloning. All constructs were sequence-verified. To generate transgenic flies, open-reading frames with epitope tags were cloned into the pUAST-attB fly expression vector and transgenes were inserted into the genome at the VK37 docking site (2L, 22A3) via PhiC31-mediated transgenesis.

Mushroom body analyses

Adult fly brains were dissected in phosphate buffered saline (PBS) and fixed in 3.7% formaldehyde in PBT (PBS+ 0.1% Triton100-X) for 15 min. Then, the brains were washed three times in PBT and blocked in PAX-DG for 1 hr at RT. The samples were later incubated with the primary antibody overnight at 4°C. After incubation, the brains were washed three times with PBT and incubated with an ALEXA Fluor secondary antibodies (Life technologies) for 2 hr at RT. After three times washes in PBT, the brains were mounted in Vectashield (Vector Labs, USA) mounting medium. The following antibodies were used: mouse anti-FasII (Developmental Studies Hybridoma Bank (DSHB), 1/50), rabbit anti-GFP (Invitrogen, 1/500). The mounted brains were imaged on a LEICA DM 6000 CS microscope coupled to a LEICA CTR 6500 confocal system and a Nikon A1-R confocal (Nikon) mounted on a Nikon inverted microscope (Nikon). The pictures were then processed using ImageJ.

Primary cortical neuron culture, virus transduction, and plasmids transfection

All experiments were done according to policies on the care and use of laboratory animals of European Communities Council Directive (2010/63). The protocols were approved by the French Research Ministry following evaluation by a specialized ethics committee (dossier number 4437). APP knock out mice were a gift from the De Strooper lab. Cortical primary neuron cultures were prepared from embryonic day 16.5 mice (APP wild or APP mutant), as described previously ([Cheng et al., 2016](#)).

Virus (pLv-pSyn1-mAPP-Flag-IRES-eGFP, pLv-pSyn1-mAPPΔCRD-Flag-IRES-eGFP, or pLv-pSyn1-eGFP) transduction was performed during seeding in 24-well plates (4x10⁵ cells/mL). Fifty μL (50 μL par well) of the adequate lentiviral dilution in the medium of interest must be ready in tubes. Seed 150 μL of the cell preparation to each well. Immediately add 50 μL of the diluted lentiviral preparation to each well (final MOI 2). Mix slowly the cells-lentivirus suspension by pipetting. Incubate 1 hr at 37°C. Finally add 800 μL of culture medium to each well and incubate for 3 additional days before any analysis.

Plasmids (pLv794_pTrip_PromSynaptin1_GFP_DeltaU3, pLv-pSyn1-MmApp-FLAG-IRES-eGFP, or pLv-pSyn1-mAPPΔCRD-FLAG-IRES-eGFP) transfection was performed at the onset of cell seeding (4x10⁵ cells/mL) in 24 wells plates with coverslip coated with PDL 24 hr before. All procedure follow

the protocol from Lipofectamine 3000 transfection reagent (ThermoFisher Catalog Number: L3000008) with little modified, each well transfection with 500 ng corresponding plasmid, medium was refreshed 5–6 hr after transfection.

Wnt and inhibitor treatment in primary neuron

Wnt5a (400 ng/ml) (645-WN-010, R and D Systems), Wnt3a (150 ng/ml) (1324-WNP-010, R and D Systems), and PBS/BSA (control) addition performed at DIV7. In all experiments related to inhibitor, cells will be treated with inhibitor 1 hr after Wnt addition (Bafilomycin A1, 100 nM, Invitrogen, 88899-55-2), LY294002 (10 μ M, Sigma, L9908) and a DMSO (0.05%DMSO in culture medium) group will be set as control. Protein or RNA samples collected after 4 hr of Wnt treatment.

A β 40/42 detection

For the A β 40/42 detection, first, culture medium refreshed with Wnt3a (50 ng/ml or 150 ng/ml) or Wnt5a (100 ng/ml or 400 ng/ml) on DIV7 primary cortical neurons. Then, supernatant was collected after 4 hr Wnt3a/5a treatment for A β detection, and refreshed with medium without Wnt3a/5a. At last, the second round supernatant collection performed after additional 24 hr culture. The procedure of A β detection is based on the protocol from V-PLEX Plus A β Peptide Panel 1 (6E10) Kit (K15200G, MSD).

Amino acids sequence of deleted CRD

Amino acids with underscore are deleted in mouse, human APP Δ CRD or APPL Δ CRD.

hAPP695 (NCBI Reference Sequence: NP_958817.1)

MLPGLALLLLAAWTARALEVPTDGNAGLLAEPQIAMFCGRLNMHMNVQNGKWSDPSGKTC
 IDTKEGILQYCOEVPELQITNVVEANQPVTIQNWCKRGRKQCKTTHPHFVPIRCLVGEFVSDAL
 LVPDKCKFLHQERMDVCETHLHWHTVAKETCSEKSTNLHDYGMLLPCGIDKFRGVEFVCCPLA
 EESDNVDSADAEEEDSDVWWGGADTDYADGSEDKVVEVAEEEEVAEVEEEEADDDDEDDEDGD
 EVEEEAEEPVEEATERTTTSIATTTTTTTSVEEVVRVPTTAASTPDAVDKYLETPGDENEHAHFQ
 KAKERLEAKHRERMSQVMREWEAERQAKNLPKADKKAVIQHFQEKVESLEQEAANERQQL
 VETHMARVEAMLNDRRLALENYITALQAVPPRRHVFNMLKKYVRAEQKDRQHTLKHFEHV
 RMVDPKAAQIRSQVMTHLRVIYERMNQSLSLLYNVPAVAEEIQDEVDLLOKEQNYSDDLAN
 MISEPRISYGNALMPSLTETKTTVELLPVNGEFLDLDLQPWHSFGADSVANTENEVEPVDAR
 PAADRGLTTRPGSGLTNIKTEEISEVKMDAEFRHDSGYEVHHQKLVFFAEDVGSNKGAIIGLMVG
 GVIATVIVITLVMLKKKQYTSIHGGVVEVDAAVTPEERHLSKMQQNGYENPTYKFFEQMQN.

MmApp (NCBI Reference Sequence: NP_031497.2)

MLPSLALLLLAAWTVRALEVPTDGNAGLLAEPQIAMFCGKLNMHMNVQNGKWESDPSGKTC
 IGTKEGILQYCOEVPELQITNVVEANQPVTIQNWCKRGRKQCKTHTHIVIPYRCLVGEFVSDALL
 VPDKCKFLHQERMDVCETHLHWHTVAKETCSEKSTNLHDYGMLLPCGIDKFRGVEFVCCPLAE
 ESDSVDSADAEEEDSDVWWGGADTDYADGGEDKVVEVAEEEEVADVEEEEADDDDEDVEDGDEV
 EEEAEEPVEEATERTTSTATTTTTTTSVEEVVRVPTTAASTPDAVDKYLETPGDENEHAHFQKAK
 ERLEAKHRERMSQVMREWEAERQAKNLPKADKKAVIQHFQEKVESLEQEAANERQQLVETHM
 ARVEAMLNDRRLALENYITALQAVPPRPHVFNMLKKYVRAEQKDRQHTLKHFEHVRMVDPKK
 AAQIRSQVMTHLRVIYERMNQSLSLLYNVPAVAEEIQDEVDLLOKEQNYSDDLANMISEPRISY
 NDALMPSLTETKTTVELLPVNGEFLDLDLQWHPFGVDSVPANTENEVEPVDARPAADRGLTT
 RPGSGLTNIKTEEISEVKMDAEFGHDSGFVVRHQKLVFFAEDVGSNKGAIIGLMVGGVIATVIVITL
 VMLKKKQYTSIHGGVVEVDAAVTPEERHLSKMQQNGYENPTYKFFEQMQN.

appl (*Drosophila melanogaster*) (NCBI Reference Sequence: NP_001245451.1)

mcaalrnlrslwvlaigtaqvqaasprwepqiavlceagqiyqpqylseegrwvtdlslkktgptclrdkmdlldyc
 kkaypnrditnivesshyqkigwcrqgalnaackgshrwkpfrcgpfqsallvpegclfdhinasrcwfpvrwn
 qtgaaacqergmqmrsfamllpcgisvfgsvfvcckphkftdeihvkktdlpvmpaaqinsandelvmndeddsn
 dsnyksdaneddddeddimgddeedmvadeaataggsntgssgdsnsqslldinaeydsgeegdnnyeedg
 ageseaeveaswdqsggakvsvlksdsspsapvapapekapvksesvtstpqlsasaaafvaansngsgtgaga

ppstaqptsdpfthfdphyehqsykrleeshrekvtrvmkdwsdleekyqdmrladpkaaqsfkqrmtarfqtstv
qaleeeegnaekhqlaamhqrvlahinqrcreamtctyqalteqppnahhvekclqklralhkdralahayrhlln
sgggpgleaaserprtlerlididravnqsmtmlkrypelsakiaqlmndyilalrskddipgsslgmseeaeagildk
yrveierkvaekerlrleakqrkeqraaerekreelrleakkvddmlksqvaeqqsqptsqsqaqqqqekslp
gkelgpdalvtaanpnlettsekdsdteygeatvsstkvtvlpvtdddavqravedvaaavahqeaepqvqhf
mthdlghressfslrrefaqhahaakegrnyvftlsfagialmaavfvgvavakwrtsrphaqgfievdqnvttthpiv
reekivpnmqingyenptykyfevke.

Quantitative real-time PCR (qRT-PCR)

Cells were lysed for RNA or protein extraction and then subjected to qRT-PCR or western blots as previously described (Liu *et al.*, 2014). The detailed sequence of each primer used in the whole study for qRT-PCR were summarized below: β -actin, sense 5'- TCCATCATGAAGTGTGACGT-3' and anti-sense 5'- GAGCAATGATCTTGATCTTCAT -3', mAPP, sense 5'- CATCCAGAACTGG TGCAAGCG-3' and anti-sense 5'- GACGGTGTGCCAGTGAAGATG -3' GAPDH, sense 5'- GC TGCCAAGGCTGTGGGCAAG-3' and anti-sense 5'- GCCTGCTTACCACCTTC -3'.

Western blots

Western blots were performed follow the user guide of Mini Gel Tank (ThermoFisher, A25977) with little modified. Briefly, Protein samples collected from total cell lysates with RIPA buffer, supernatant were collected after centrifugation, denatured samples were loaded separated on the 4–12% polyacrylamide gels (SDS-PAGE) (ThermoFisher, NW04122BOX) and then transferred to the 0.42 μ m nitrocellulose membranes, blots visualization performed after primary and secondary antibody incubation.

Immunoprecipitation

Human embryonic kidney (HEK293) cells (provided from Dr. Marie-Claude Potier) were purchased from ATCC, regularly mycoplasma test performed by the CELIS core facility of ICM. For the immunoprecipitation experiments, HEK293 in 10 cm dish (70% confluent) were transfected with pCDNA3-MmApp-FLAG-IRES-eGFP, pCDNA3-mAPP Δ CRD-FLAG-IRES-eGFP, pCDNA3-Wnt5a-myc, pCDNA-Wnt3A-V5 or co-transfected APP or APP Δ CRD with Wnt3a or Wnt5a. Three days after transfection, cells were collected with NP-40 lysis buffer, then sample supernatant was collected after >12000 rpm centrifugation for 20 min at 4°C, 450 μ l supernatant was incubated with primary antibody overnight at 4°C, then Protein G sepharose beads (Thermo Fisher Scientific) were added to the sample to capture protein-antibody complex by rotating 2 hr at room temperature, then washed four times with the lysis buffer, and resuspended with loading buffer then denatured at 95 degree for 10 min, blots visualized after western blot procedure as described before.

Immunofluorescence

At DIV 7, cultured primary neurons in 24 wells were washed once with 1X PBS, then fixed in 4% paraformaldehyde (PFA) in PBS at room temperature (RT) for 10 min. After three times washing with 1X PBS, cells were blocked with 10% normal donkey or goat serum in 1 X PBS for 30 min at RT followed by three times washing in 1 X PBS. Thereafter, cells were incubated with primary antibodies diluted in 1 X PBS containing 1% normal donkey or goat serum for 2–3 hr at RT. three times washing with 1 X PBS, incubated with appropriate secondary antibodies conjugated with Alexa Fluor 488, Alexa Fluor 555, or Alexa Fluor 647 (1:500, Invitrogen) in 1 X PBS containing 1% normal donkey or goat serum for 1 hr at RT. Washed with 1 X PBS for three times, then counterstained the slides with DAPI (1:2000, Sigma) and mounted by using Vectashield (Vector) after rinsing. Primary antibodies used in this study were rabbit anti-APP (1:100, Synaptic Systems, 127 003), mouse anti-rab5 (1:100, Synaptic Systems, 108011), mouse anti-rab11a (1:20, Santa Cruz, sc-166523), mouse anti- Golgin-97 (1:100, Invitrogen, A-21270), rat anti-Lamp1 (1:20, Santa Cruz, sc-19992). After staining, images were obtained by using confocal microscope (Olympus FV-1200 or Leica SP8). The percentage of APP or APP- Δ CRD co-localizing with rab5, rab11, Golgin-97 and Lamp1 was calculated using JACOP (Bolte and Cordelières, 2006).

Statistical analyses

Statistical analyses were performed using GraphPad Prism software (GraphPad Software Inc, La Jolla, CA, USA). Differences between groups were compared using the Student's t test, One-way ANOVA and Mann Whitney two-sample test (two-tail) as appropriate.

Acknowledgements

We thank Dr. Radoslaw Ejsmont for writing the co-localization macro, Natalia Danda for the construction of the plasmids used in this work, Drs. Ariane Ramaekers, Natalia Mora Garcia, Gerit Linne-weber, Simon Weinberger and Guangda Liu for helpful discussions. We thank Drs. Zeynep Kalender Atak and Marina Naval Sanchez for support on the statistical analysis of the data and Dr. Jean-Maurice Dura for fly lines. Mouse breeding work was conducted at the PHENO-ICMice facility. The Core is supported by 2 Investissements d'Avenir grants (ANR-10- IAIHU-06 and ANR-11-INBS-0011-NeurATRIS) and the 'Fondation pour la Recherche Médicale'. Primary neuron culture work was carried out at the CELIS core facility with support from Program Investissements d'Avenir (ANR-10-IAIHU-06). Light microscopy was carried out at the ICM.Quant facility. We thank all core technical staff involved. We thank Philippe Ravassard for providing the pSYN lentiviral vector backbone and Blandise Bonnamy and Clementine Ripoll from iVECTOR core facility for technical assistance and production of the lentiviral vectors. This work was supported by Fonds Wetenschappelijk Onderzoeks (FWO) grants G.0543.08, G.0680.10, G.0681.10 and G.0503.12, the program 'Investissements d'avenir' ANR-10-IAIHU-06, the Einstein-BIH program, the Neuro-Glia Foundation, a Sorbonne Université Emergence grant, an Allen Distinguished Investigator Award and the Roger De Spoelberch Foundation Prize (to BAH), ANR-12-MALZ-0004 grant (to MCP), the Vlaams Instituut voor Biotechnologie and the Methusalem grants from KU Leuven (to BDS and BAH), the Nederlandse Organisatie voor Wetenschappelijk Onderzoek (NWO; ZonMw TOP grant 40-00812-98-10058) and the Hersenstichting Nederland [HS 2011(1)–46] (to LGF), a doctoral fellowship from the Centre National de Recherche Scientifique Libanais (to MN) and Chinese Scholarship Council fellowships (to TZ and TL). The authors declare no competing financial interests.

Additional information

Funding

Funder	Grant reference number	Author
China Scholarship Council		Tengyuan Liu
Hersenstichting	HS 2011(1)-46	Lee Fradkin
Lebanese National Council for Scientific Research		Maya Nicolas
Vlaams Instituut voor Biotechnologie		Bart De Strooper Bassem A Hassan
Fondation Roger de Spoelberch	1911001IN	Bassem A Hassan
Agence Nationale de la Recherche	ANR-10-IAIHU-06	Marie-Claude Potier Bassem A Hassan
Fonds Wetenschappelijk Onderzoek	G.0543.08	Bassem A Hassan
Neuron-Glia Foundation	2003009NA	Bassem A Hassan
KU Leuven	Methusalem	Bart De Strooper Bassem A Hassan
Nederlandse Organisatie voor Wetenschappelijk Onderzoek	40-00812-98-10058	Lee Fradkin
Fonds Wetenschappelijk Onderzoek	G.0680.10	Bassem A Hassan
Fonds Wetenschappelijk Onderzoek	G.0681.10	Bassem A Hassan

derzoek

Fonds Wetenschappelijk Onderzoek	G.0503.12	Bassem A Hassan
Agence Nationale de la Recherche	ANR-11-INBS-0011-NeurATRIS	Marie-Claude Potier Bassem A Hassan
Agence Nationale de la Recherche	ANR-12-MALZ-0004	Marie-Claude Potier Bassem A Hassan

The funders had no role in study design, data collection and interpretation, or the decision to submit the work for publication.

Author contributions

Tengyuan Liu, Conceptualization, Formal analysis, Investigation, Methodology, Writing - original draft, Writing - review and editing; Tingting Zhang, Formal analysis, Investigation, Methodology; Maya Nicolas, Conceptualization, Formal analysis, Investigation, Methodology, Writing - original draft; Lydie Boussicault, Heather Rice, Investigation, Methodology; Alessia Soldano, Conceptualization, Investigation; Annelies Claeys, Iveta Petrova, Investigation; Lee Fradkin, Conceptualization, Supervision, Funding acquisition; Bart De Strooper, Marie-Claude Potier, Supervision, Funding acquisition; Bassem A Hassan, Conceptualization, Supervision, Funding acquisition, Writing - original draft, Project administration, Writing - review and editing

Author ORCIDs

Maya Nicolas  <https://orcid.org/0000-0002-7148-6357>

Alessia Soldano  <http://orcid.org/0000-0002-3120-9929>

Bart De Strooper  <http://orcid.org/0000-0001-5455-5819>

Marie-Claude Potier  <http://orcid.org/0000-0003-2462-7150>

Bassem A Hassan  <https://orcid.org/0000-0001-9533-4908>

Ethics

Animal experimentation: All experiments were done according to policies on the care and use of laboratory animals of European Communities Council Directive (2010/63). The protocols were approved by the French Research Ministry following evaluation by a specialized ethics committee (dossier number 4437).

Decision letter and Author response

Decision letter <https://doi.org/10.7554/eLife.69199.sa1>

Author response <https://doi.org/10.7554/eLife.69199.sa2>

Additional files

Supplementary files

- Supplementary file 1. Genetic interaction between Wnt5 and Vang. The table lists the penetrance of the phenotype and the number of brains analyzed in the Vang-Wnt5 genetic interaction experiment.
- Transparent reporting form

Data availability

No new datasets were generated in this study.

References

Ables JL, Breunig JJ, Eisch AJ, Rakic P. 2011. Not(ch) just development: notch signalling in the adult brain. *Nature Reviews Neuroscience* **12**:269–283. DOI: <https://doi.org/10.1038/nrn3024>, PMID: 21505516

- Araki W, Kitaguchi N, Tokushima Y, Ishii K, Aratake H, Shimohama S, Nakamura S, Kimura J. 1991. Trophic effect of beta-amyloid precursor protein on cerebral cortical neurons in culture. *Biochemical and Biophysical Research Communications* **181**:265–271. DOI: [https://doi.org/10.1016/S0006-291X\(05\)81412-3](https://doi.org/10.1016/S0006-291X(05)81412-3), PMID: 1958195
- Barnes AP, Polleux F. 2009. Establishment of axon-dendrite polarity in developing neurons. *Annual Review of Neuroscience* **32**:347–381. DOI: <https://doi.org/10.1146/annurev.neuro.31.060407.125536>, PMID: 19400726
- Billnitzer AJ, Barskaya I, Yin C, Perez RG. 2013. APP independent and dependent effects on neurite outgrowth are modulated by the receptor associated protein (RAP). *Journal of Neurochemistry* **124**:123–132. DOI: <https://doi.org/10.1111/jnc.12051>, PMID: 23061396
- Bolte S, Cordelières FP. 2006. A guided tour into subcellular colocalization analysis in light microscopy. *Journal of Microscopy* **224**:213–232. DOI: <https://doi.org/10.1111/j.1365-2818.2006.01706.x>, PMID: 17210054
- Bush AI, Multhaup G, Moir RD, Williamson TG, Small DH, Rumble B, Pollwein P, Beyreuther K, Masters CL. 1993. A novel zinc(II) binding site modulates the function of the beta A4 amyloid protein precursor of Alzheimer's disease. *Journal of Biological Chemistry* **268**:16109–16112. DOI: [https://doi.org/10.1016/S0021-9258\(19\)85394-2](https://doi.org/10.1016/S0021-9258(19)85394-2)
- Cassar M, Kretschmar D. 2016. Analysis of amyloid precursor protein function in *Drosophila melanogaster*. *Frontiers in Molecular Neuroscience* **9**:61. DOI: <https://doi.org/10.3389/fnmol.2016.00061>, PMID: 27507933
- Chang KA, Kim HS, Ha TY, Ha JW, Shin KY, Jeong YH, Lee JP, Park CH, Kim S, Baik TK, Suh YH. 2006. Phosphorylation of amyloid precursor protein (APP) at Thr668 regulates the nuclear translocation of the APP intracellular domain and induces neurodegeneration. *Molecular and Cellular Biology* **26**:4327–4338. DOI: <https://doi.org/10.1128/MCB.02393-05>, PMID: 16705182
- Chen CD, Oh SY, Hinman JD, Abraham CR. 2006. Visualization of APP dimerization and APP-Notch2 heterodimerization in living cells using bimolecular fluorescence complementation. *Journal of Neurochemistry* **97**:30–43. DOI: <https://doi.org/10.1111/j.1471-4159.2006.03705.x>, PMID: 16515557
- Cheng A, Yang Y, Zhou Y, Maharana C, Lu D, Peng W, Liu Y, Wan R, Marosi K, Misiak M, Bohr VA, Mattson MP. 2016. Mitochondrial SIRT3 mediates adaptive responses of neurons to exercise and metabolic and excitatory challenges. *Cell Metabolism* **23**:128–142. DOI: <https://doi.org/10.1016/j.cmet.2015.10.013>, PMID: 26698917
- Coburger I, Dahms SO, Roeser D, Gührs KH, Hortschansky P, Than ME. 2013. Analysis of the overall structure of the multi-domain amyloid precursor protein (APP). *PLOS ONE* **8**:e81926. DOI: <https://doi.org/10.1371/journal.pone.0081926>, PMID: 24324731
- Coronel R, Bernabeu-Zornoza A, Palmer C, Muñoz-Moreno M, Zambrano A, Cano E, Liste I. 2018. Role of amyloid precursor protein (APP) and its derivatives in the biology and cell fate specification of neural stem cells. *Molecular Neurobiology* **55**:7107–7117. DOI: <https://doi.org/10.1007/s12035-018-0914-2>, PMID: 29383688
- Dann CE, Hsieh JC, Rattner A, Sharma D, Nathans J, Leahy DJ. 2001. Insights into wnt binding and signalling from the structures of two frizzled cysteine-rich domains. *Nature* **412**:86–90. DOI: <https://doi.org/10.1038/35083601>, PMID: 11452312
- Deyts C, Thinakaran G, Parent AT. 2016. APP receptor? to be or not to be. *Trends in Pharmacological Sciences* **37**:390–411. DOI: <https://doi.org/10.1016/j.tips.2016.01.005>, PMID: 26837733
- Dotti CG, Sullivan CA, Banker GA. 1988. The establishment of polarity by hippocampal neurons in culture. *The Journal of Neuroscience* **8**:1454–1468. DOI: <https://doi.org/10.1523/JNEUROSCI.08-04-01454.1988>, PMID: 3282038
- Eisenmann DM. 2005. Wnt signaling. *WormBook* **1**:1–17. DOI: <https://doi.org/10.1895/wormbook.1.7.1>, PMID: 18050402
- El Ayadi A, Stieren ES, Barral JM, Boehning D. 2012. Ubiquitin-1 regulates amyloid precursor protein maturation and degradation by stimulating K63-linked polyubiquitination of lysine 688. *PNAS* **109**:13416–13421. DOI: <https://doi.org/10.1073/pnas.1206786109>, PMID: 22847417
- Elliott C, Rojo AI, Ribe E, Broadstock M, Xia W, Morin P, Semenov M, Baillie G, Cuadrado A, Al-Shawi R, Ballard CG, Simons P, Killick R. 2018. A role for APP in wnt signalling links synapse loss with β -amyloid production. *Translational Psychiatry* **8**:179. DOI: <https://doi.org/10.1038/s41398-018-0231-6>, PMID: 30232325
- Grillenzoni N, Flandre A, Lasbleiz C, Dura JM. 2007. Respective roles of the DRL receptor and its ligand WNT5 in *Drosophila* mushroom body development. *Development* **134**:3089–3097. DOI: <https://doi.org/10.1242/dev.02876>, PMID: 17652353
- Haass C, Kaether C, Thinakaran G, Sisodia S. 2012. Trafficking and proteolytic processing of APP. *Cold Spring Harbor Perspectives in Medicine* **2**:a006270. DOI: <https://doi.org/10.1101/cshperspect.a006270>, PMID: 22553493
- Heisenberg M. 2003. Mushroom body memoir: from maps to models. *Nature Reviews Neuroscience* **4**:266–275. DOI: <https://doi.org/10.1038/nrn1074>, PMID: 12671643
- Hoe HS, Lee KJ, Carney RS, Lee J, Markova A, Lee JY, Howell BW, Hyman BT, Pak DT, Bu G, Rebeck GW. 2009. Interaction of reelin with amyloid precursor protein promotes neurite outgrowth. *Journal of Neuroscience* **29**:7459–7473. DOI: <https://doi.org/10.1523/JNEUROSCI.4872-08.2009>, PMID: 19515914
- Hunter S, Brayne C. 2012. Relationships between the amyloid precursor protein and its various proteolytic fragments and neuronal systems. *Alzheimer's Research & Therapy* **4**:10. DOI: <https://doi.org/10.1186/alzrt108>, PMID: 22498202
- Kaden D, Voigt P, Munter LM, Bobowski KD, Schaefer M, Multhaup G. 2009. Subcellular localization and dimerization of APLP1 are strikingly different from APP and APLP2. *Journal of Cell Science* **122**:368–377. DOI: <https://doi.org/10.1242/jcs.034058>, PMID: 19126676

- Kang J**, Lemaire HG, Unterbeck A, Salbaum JM, Masters CL, Grzeschik KH, Multhaup G, Beyreuther K, Müller-Hill B. 1987. The precursor of Alzheimer's disease amyloid A4 protein resembles a cell-surface receptor. *Nature* **325**:733–736. DOI: <https://doi.org/10.1038/325733a0>, PMID: 2881207
- Liu T**, Zhang T, Yu H, Shen H, Xia W. 2014. Adjudin protects against cerebral ischemia reperfusion injury by inhibition of neuroinflammation and blood-brain barrier disruption. *Journal of Neuroinflammation* **11**:107. DOI: <https://doi.org/10.1186/1742-2094-11-107>
- Müller UC**, Zheng H. 2012. Physiological functions of APP family proteins. *Cold Spring Harbor Perspectives in Medicine* **2**:a006288. DOI: <https://doi.org/10.1101/cshperspect.a006288>, PMID: 22355794
- Mulligan KA**, Chetty BN. 2012. Wnt signaling in vertebrate neural development and function. *Journal of Neuroimmune Pharmacology* **7**:774–787. DOI: <https://doi.org/10.1007/s11481-012-9404-x>, PMID: 23015196
- Nicolas M**, Hassan BA. 2014. Amyloid precursor protein and neural development. *Development* **141**:2543–2548. DOI: <https://doi.org/10.1242/dev.108712>, PMID: 24961795
- Niehrs C**. 2012. The complex world of WNT receptor signalling. *Nature Reviews Molecular Cell Biology* **13**:767–779. DOI: <https://doi.org/10.1038/nrm3470>
- Ninomiya H**, Roch JM, Sundsmo MP, Otero DA, Saitoh T. 1993. Amino acid sequence RERMS represents the active domain of amyloid beta/A4 protein precursor that promotes fibroblast growth. *Journal of Cell Biology* **121**:879–886. DOI: <https://doi.org/10.1083/jcb.121.4.879>
- Oishi I**, Suzuki H, Onishi N, Takada R, Kani S, Ohkawara B, Koshida I, Suzuki K, Yamada G, Schwabe GC, Mundlos S, Shibuya H, Takada S, Minami Y. 2003. The receptor tyrosine kinase Ror2 is involved in non-canonical Wnt5a/JNK signalling pathway. *Genes to Cells* **8**:645–654. DOI: <https://doi.org/10.1046/j.1365-2443.2003.00662.x>, PMID: 12839624
- Ott MO**, Bullock SL. 2001. A gene trap insertion reveals that amyloid precursor protein expression is a very early event in murine embryogenesis. *Development Genes and Evolution* **211**:355–357. DOI: <https://doi.org/10.1007/s004270100158>, PMID: 11466532
- Panegyres PK**, Atkins ER. 2011. The Functions of the Amyloid Precursor Protein Gene and Its Derivative Peptides: I Molecular Biology and Metabolic Processing. *Neuroscience and Medicine* **02**:120–131. DOI: <https://doi.org/10.4236/nm.2011.22018>
- Parr C**, Mirzaei N, Christian M, Sastre M. 2015. Activation of the wnt/ β -catenin pathway represses the transcription of the β -amyloid precursor protein cleaving enzyme (BACE1) via binding of T-cell factor-4 to BACE1 promoter. *The FASEB Journal* **29**:623–635. DOI: <https://doi.org/10.1096/fj.14-253211>, PMID: 25384422
- Perez RG**, Zheng H, Van der Ploeg LH, Koo EH. 1997. The beta-amyloid precursor protein of Alzheimer's disease enhances neuron viability and modulates neuronal polarity. *The Journal of Neuroscience* **17**:9407–9414. DOI: <https://doi.org/10.1523/JNEUROSCI.17-24-09407.1997>, PMID: 9390996
- Pietrzik CU**, Yoon IS, Jaeger S, Busse T, Weggen S, Koo EH. 2004. FE65 constitutes the functional link between the low-density lipoprotein receptor-related protein and the amyloid precursor protein. *Journal of Neuroscience* **24**:4259–4265. DOI: <https://doi.org/10.1523/JNEUROSCI.5451-03.2004>, PMID: 15115822
- Polleux F**, Snider W. 2010. Initiating and growing an axon. *Cold Spring Harbor Perspectives in Biology* **2**:a001925. DOI: <https://doi.org/10.1101/cshperspect.a001925>, PMID: 20452947
- Preat T**, Goguel V. 2016. Role of *Drosophila* amyloid precursor protein in memory formation. *Frontiers in Molecular Neuroscience* **9**:142. DOI: <https://doi.org/10.3389/fnmol.2016.00142>, PMID: 28008309
- Reinhard C**, Hébert SS, De Strooper B. 2005. The amyloid-beta precursor protein: integrating structure with biological function. *The EMBO Journal* **24**:3996–4006. DOI: <https://doi.org/10.1038/sj.emboj.7600860>, PMID: 16252002
- Rossjohn J**, Cappai R, Feil SC, Henry A, McKinstry WJ, Galatis D, Hesse L, Multhaup G, Beyreuther K, Masters CL, Parker MW. 1999. Crystal structure of the nterminal, growth factor-like domain of alzheimer amyloid precursor protein. *Nature Structural Biology* **6**:327–331. DOI: <https://doi.org/10.1038/7562>, PMID: 10201399
- Rosso SB**, Inestrosa NC. 2013. WNT signaling in neuronal maturation and synaptogenesis. *Frontiers in Cellular Neuroscience* **7**:103. DOI: <https://doi.org/10.3389/fncel.2013.00103>, PMID: 23847469
- Salbaum JM**, Ruddle FH. 1994. Embryonic expression pattern of amyloid protein precursor suggests a role in differentiation of specific subsets of neurons. *Journal of Experimental Zoology* **269**:116–127. DOI: <https://doi.org/10.1002/jez.1402690205>
- Sarasa M**, Sorribas V, Terradao J, Climent S, Palacios JM, Mengod G. 2000. Alzheimer beta-amyloid precursor proteins display specific patterns of expression during embryogenesis. *Mechanisms of Development* **94**:233–236. DOI: [https://doi.org/10.1016/S0925-4773\(00\)00297-5](https://doi.org/10.1016/S0925-4773(00)00297-5), PMID: 10842078
- Selkoe DJ**, Hardy J. 2016. The amyloid hypothesis of Alzheimer's disease at 25 years. *EMBO Molecular Medicine* **8**:595–608. DOI: <https://doi.org/10.15252/emmm.201606210>, PMID: 27025652
- Sellers KJ**, Elliott C, Jackson J, Ghosh A, Ribe E, Rojo AI, Jarosz-Griffiths HH, Watson IA, Xia W, Semenov M, Morin P, Hooper NM, Porter R, Preston J, Al-Shawi R, Baillie G, Lovestone S, Cuadrado A, Harte M, Simons P, et al. 2018. Amyloid β synaptotoxicity is Wnt-PCP dependent and blocked by fasudil. *Alzheimer's & Dementia* **14**:306–317. DOI: <https://doi.org/10.1016/j.jalz.2017.09.008>, PMID: 29055813
- Shariati SA**, De Strooper B. 2013. Redundancy and divergence in the amyloid precursor protein family. *FEBS Letters* **587**:2036–2045. DOI: <https://doi.org/10.1016/j.febslet.2013.05.026>, PMID: 23707420
- Shimizu K**, Sato M, Tabata T. 2011. The Wnt5/planar cell polarity pathway regulates axonal development of the *Drosophila* mushroom body neuron. *Journal of Neuroscience* **31**:4944–4954. DOI: <https://doi.org/10.1523/JNEUROSCI.0154-11.2011>, PMID: 21451033
- Small DH**, Nurcombe V, Reed G, Clarris H, Moir R, Beyreuther K, Masters CL. 1994. A heparin-binding domain in the amyloid protein precursor of Alzheimer's disease is involved in the regulation of neurite outgrowth. *The*

- Journal of Neuroscience* **14**:2117–2127. DOI: <https://doi.org/10.1523/JNEUROSCI.14-04-02117.1994>, PMID: 8158260
- Soldano A**, Okray Z, Janovska P, Tmejová K, Reynaud E, Claeys A, Yan J, Atak ZK, De Strooper B, Dura JM, Bryja V, Hassan BA. 2013. The *Drosophila* homologue of the amyloid precursor protein is a conserved modulator of wnt PCP signaling. *PLOS Biology* **11**:e1001562. DOI: <https://doi.org/10.1371/journal.pbio.1001562>, PMID: 23690751
- Soldano A**, Hassan BA. 2014. Beyond pathology: app, brain development and Alzheimer's disease. *Current Opinion in Neurobiology* **27**:61–67. DOI: <https://doi.org/10.1016/j.conb.2014.02.003>, PMID: 24632309
- Southam KA**, Stennard F, Pavez C, Small DH. 2019. Knockout of amyloid β protein precursor (APP) Expression alters synaptogenesis, neurite branching and axonal morphology of hippocampal neurons. *Neurochemical Research* **44**:1346–1355. DOI: <https://doi.org/10.1007/s11064-018-2512-0>, PMID: 29572646
- Stahl R**, Schilling S, Soba P, Rupp C, Hartmann T, Wagner K, Merdes G, Eggert S, Kins S. 2014. Shedding of APP limits its synaptogenic activity and cell adhesion properties. *Frontiers in Cellular Neuroscience* **8**:410. DOI: <https://doi.org/10.3389/fncel.2014.00410>, PMID: 25520622
- Tapia-Rojas C**, Burgos PV, Inestrosa NC. 2016. Inhibition of wnt signaling induces amyloidogenic processing of amyloid precursor protein and the production and aggregation of Amyloid- β (A β)₄₂ peptides. *Journal of Neurochemistry* **139**:1175–1191. DOI: <https://doi.org/10.1111/jnc.13873>, PMID: 27778356
- Vagnozzi AN**, Praticò D. 2019. Endosomal sorting and trafficking, the retromer complex and neurodegeneration. *Molecular Psychiatry* **24**:857–868. DOI: <https://doi.org/10.1038/s41380-018-0221-3>, PMID: 30120416
- van der Kant R**, Goldstein LS. 2015. Cellular functions of the amyloid precursor protein from development to dementia. *Developmental Cell* **32**:502–515. DOI: <https://doi.org/10.1016/j.devcel.2015.01.022>, PMID: 25710536
- Wong HH**, Lin JQ, Ströhl F, Roque CG, Cioni JM, Cagnetta R, Turner-Bridger B, Laine RF, Harris WA, Kaminski CF, Holt CE. 2017. RNA docking and local translation regulate Site-Specific axon remodeling in Vivo. *Neuron* **95**:852–868. DOI: <https://doi.org/10.1016/j.neuron.2017.07.016>, PMID: 28781168
- Young-Pearse TL**, Chen AC, Chang R, Marquez C, Selkoe DJ. 2008. Secreted APP regulates the function of full-length APP in neurite outgrowth through interaction with integrin beta1. *Neural Development* **3**:15. DOI: <https://doi.org/10.1186/1749-8104-3-15>, PMID: 18573216
- Yuksel M**, Tacal O. 2019. Trafficking and proteolytic processing of amyloid precursor protein and secretases in Alzheimer's disease development: An up-to-date review. *European Journal of Pharmacology* **856**:172415. DOI: <https://doi.org/10.1016/j.ejphar.2019.172415>, PMID: 31132354